**US Army Corps
of Engineers**
Waterways Experiment
Station

AD-A282 732

Design of Regional Wave Monitoring Networks: A Case Study for the Southern California Bight

by   William C. O'Reilly
     Scripps Institution of Oceanography

     David D. McGehee

DTIC
ELECTE
JUL 27 1994
S G D

WES

94-23794

DTIC QUALITY INSPECTED 5

94 7 26 1 13

The contents of this report are not to be used for advertising, publication, or promotional purposes. Citation of trade names does not constitute an official endorsement or approval of the use of such commercial products.

Design of Regional Wave Monitoring Networks: A Case Study for the Southern California Bight

by William C. O'Reilly

Scripps Institution of Oceanography
University of California, San Diego
La Jolla, CA 92093

David D. McGehee

U.S. Army Corps of Engineers
Waterways Experiment Station
3909 Halls Ferry Road
Vicksburg, MS 39180-6199

Accesion For		
NTIS CRA&I		☒
DTIC TAB		☐
Unannounced		☐
Justification		
By		
Dist. ibution /		
Availability Codes		
Dist	Avail and / or Special	
A-1		

Final report

Approved for public release; distribution is unlimited

**US Army Corps
of Engineers**
Waterways Experiment
Station

Contents

Preface

1 Introduction

The U.S. Army Corps of Engineers and the California Department of Boating and Waterways (CDBW) need reliable, long-term wave measurements for use in planning, designing, and operating coastal projects. Design wave conditions, usually expressed in terms of return intervals, are obtained through extremal analysis of wave histories. The confidence in these projects drops as the desired return interval exceeds about twice the length of the historical record. However, there is seldom time between the inception of a project and the point when design details are finalized to collect sufficiently long wave histories. A commitment is needed to obtain the required long-term measurements in advance of specific project planning. Wave hindcasts - which are made possible by long-term meteorological observations - such as the successful Wave Information Studies (WIS) conducted at the U.S. Army Engineer Waterways Experiment Station, Coastal Engineering Research Center, are another approach to this need, but wave measurements are still required for their validation. Another need for wave data is accurate quantification of conditions during specific events that result in damage to structures or delays in operations. Finally, laboratory and analytical research into the physics of wave generation, propagation, and transformation require measurements for calibration and verification.

The Corps and the CDBW established the Coastal Data Information Program (CDIP) with the goal of collecting wave data at sufficient spatial and temporal density to meet these needs for the entire U.S. Pacific coastline. CDIP is a network of wave gauges operated by the University of California at San Diego Scripps Institution of Oceanography (Flick et al. 1993). To date, the density of wave observations is inadequate to sufficiently monitor the U.S. coastline, and any site selected for monitoring is a valuable addition to our knowledge. As the number of stations increases, it is imperative that locations be efficiently distributed to avoid collecting redundant data.

The overall goal of the report is to provide preliminary guidance and recommendations for the future study and implementation of regional wave monitoring networks. The technical background upon which the report is based, and extensive references to past work, are given in O'Reilly (1991). The focus here is on potential engineering applications.

It is important to note at the outset that the methodologies described in this report were developed to study relatively long-period waves (swell) arriving in

southern California from distant storms. When appropriate, the discussion has been generalized to include locally generated seas. However, the fundamental considerations in optimizing a network of gauges to monitor swell versus local seas are believed to be quite distinct. Differences in swell wave conditions between a network's measurement stations are primarily due to variations in wave propagation over the regional bathymetry. For local seas, differences between stations are more likely to be dominated by variations in the regional wind field. A complete methodology for designing networks must eventually find a balance between these two competing criteria.

Regional wave monitoring is defined here as the use of wave data collected at a limited number of locations to estimate wave conditions throughout an entire coastal region. The term "wave conditions" refers to wave parameters needed for engineering design and planning (e.g. significant wave height, peak wave period, radiation stress, etc.). A "coastal region" is defined as an area where the directional spectra for incident swell can be approximated as homogeneous along its deepwater boundary. Historically, shallow-water wave measurements have been collected primarily for site-specific purposes. Although data with regional applicability are obviously desirable, relatively little research has been done on the design of regional wave networks.

Relating wave measurements (and/or hindcasts) to regional wave conditions requires some type of *estimation theory*. Possible estimation methods are discussed, including simple linear interpolation between adjacent gauges and sophisticated schemes using numerical wave propagation models. An objective technique for designing optimal wave gauge networks is also described, providing a conceptual framework for addressing regional monitoring issues such as how many, where, and what types of measurement should be made.

The authors strongly recommend that the utility of deepwater directional buoys, in combination with numerical wave models, be closely examined for regional wave monitoring along exposed coastlines with relatively simple bathymetry. Directional buoys are sometimes inadequate for coastal regions with complex bathymetry, and shallow-water measurements must be an integral part of these networks. Optimal shallow-water gauge networks provide an objectively rigorous field test of regional wave prediction schemes on both simple and complex bathymetry.

2

2 Measurement and Estimation Theory Uncertainty

Wave parameters of interest are defined as wave energy and the first four directional moments of wave spectra at locations outside the surf zone. This definition corresponds to what can be obtained directly from slope array or pitch-and-roll buoy measurements, and also to the level of detailed wave information needed for many engineering applications.

Uncertainty in wave measurements is primarily statistical, caused by the limited duration of wave records and/or the nonstationarity of the wave field. Smaller errors arise from sensor inaccuracies, buoy calibration errors, etc. If an *exact* linear estimator theory related the various local measurements to the regional wave field, and the gauges were far enough apart to be statistically independent, then the regional estimates would theoretically have less statistical uncertainty than an individual measurement. For example, if the exact theory were a simple correlation scheme where the total energy at site B was the average of the energies at sites A and C, then the statistical uncertainty would actually be less at B than A or C. However, the estimation theories are far from exact, and quantifying the estimator errors is one of the more difficult aspects of designing a monitoring program. The many errors associated with estimating wave conditions at one location from measurements at other sites are usually understood only to the extent that these errors are larger than statistical and instrumental errors. The approach taken here is to assume that the estimation theory, whatever it may be, is exact for the purpose of designing a network. Field experiments are needed to quantify the errors and thus ultimately validate the estimation scheme.

3   Estimation Theories

Methods for relating specific wave measurements to wave conditions at other sites can be crudely divided into the four categories discussed below.

Interpolation Methods

The simplest (and most costly) approach to regional monitoring is to instrument the entire coastline, with the spacing between gauges small enough such that wave conditions change only a small amount between gauges. In this case, wave conditions between gauges could, by definition, be accurately estimated through linear interpolation. Along broad reaches of open coastline the gauge spacing might be quite large, but near very complicated bathymetry, for example, near submarine canyons, this spacing could be reduced to less than 100 m. In general, the number of required gauges is prohibitively large, and monitoring networks based on simple interpolation methods have very limited practical value.

Correlation Methods

A more general form of linear interpolation utilizes empirically determined linear correlations between wave parameters at different wave gauges, or between deep-ocean wave parameters and shallow-water conditions. Wave gauges at locations where wave conditions are highly correlated with other (not necessarily spatially adjacent) gauge sites can be eliminated from the network. However, linear correlation methods have not been successful on complex bathymetry (e.g. Southern California) because the relationship between wave conditions at two different sites, a very complicated function of the deep-ocean directional spectrum, cannot be well characterized by a linear equation with just a few variables, such as the peak wave frequency and direction of a deep-ocean wave event. With simple bathymetry and wave conditions (single, narrow directional peaks), strong correlations might be found between directional buoy measurements in deep water and shallow-water array measurements. However, determining the correlations in this case is essentially equivalent to empirically (and at considerable expense) finding the refraction and shoaling coefficients of simple linear wave propagation theory. In addition, this

4

empirical approach requires that every location of interest be occupied by a gauge for a long duration in order to establish the correlations. Correlation methods may have some use in site-specific problems, but are not considered viable for regional wave monitoring in general.

The motivation behind correlation methods is to avoid making long-term measurements of highly correlated, or redundant, wave information. In Chapter 5, it will be shown how numerical wave models, linear programming, and optimization techniques can be combined to select gauge locations which minimize redundancy.

Numerical Wave Models

Numerical wave propagation models can be invaluable in the design and operation of regional monitoring networks. A straightforward example is using a single directional buoy in deep water to initialize a wave propagation model that predicts the wave field at shoreward locations. If the wave model were exact and the buoy measurements completely defined the deepwater directional wave spectrum, then the coastal wave field could be accurately estimated with no shallow-water measurements at all. However, neither assumption is in general satisfied. The wave models rely on many simplifying assumptions and the conditions under which the waves propagate (i.e. bathymetry, currents) are imprecisely known (see Chapter 2). Furthermore, pitch-and-roll buoys and two-component slope arrays are fundamentally low-resolution instruments relative to multi-element arrays. An infinite number of directional spectra, some of them markedly different in shape and equally plausible, can exactly fit the same slope data.

Despite these limitations, various methods for assigning directional distributions to pitch-and-roll data (e.g. Maximum Likelihood Method, MLM, or Maximum Entropy Method, MEM), in conjunction with available wave propagation models, may prove adequate for some regions of U.S. coastline. The Southern California Wave Experiment, conducted over the winter of 1991-1992, was designed to test this approach. Two linear wave propagation models (O'Reilly and Guza 1992) were initialized with MEM estimates of the offshore spectrum obtained from deepwater directional wave gauges within the Bight.

The buoy-wave propagation models provide good predictions of Bight-wide wave conditions for the more open sections of coastline. Simple bathymetry reduces the sensitivity of coastal wave conditions to details of the offshore directional spectrum, and comparisons with shallow-water measurements verified the utility of this straightforward monitoring approach in these cases. At the most highly sheltered and topographically complex shallow-water sites, the limitations of this approach were evident.

The combined buoy-wave propagation estimator is relatively cheap because a single buoy serves a relatively large stretch of coastline. The spacing of the offshore buoys should be such that the deepwater directional spectrum varies slowly between them. This spacing would presumably be some fraction of the

length scale of typical storm events, and is best addressed through historical data, from hindcast data, such as provided by the WIS, and future field experiments. The buoy-wave propagation monitoring scheme should be extensively tested, and concurrent data from offshore National Oceanic and Atmospheric Administration (NOAA) buoys and shallow-water stations may already exist for many sections of the U.S. coastline. Where directional buoys prove sufficient, shallow-water instrumentation would be used primarily for site-specific problems requiring exceptionally high accuracy, or for monitoring local seas that are generated between the buoy and the coast.

In addition to propagating waves from offshore to onshore, numerical wave models can also be used to "back out" shallow-water directional measurements to deep water. These deepwater directional spectra can in turn be used to predict shallow-water conditions elsewhere, as described above. At first glance a shallow-water directional buoy has value equal to a deepwater buoy. However, this is not the case because refraction columnates low-frequency deep-ocean waves to a narrow band nearly normal to the beach in shallow water. Swell with a relatively broad directional spread in deep water is much narrower in shallow water, and detail in the shallow spectrum cannot be well resolved with a slope array or pitch-and-roll buoy. Owing to this resolution problem alone, there is greater uncertainty in deepwater directional spectra obtained by backing out shallow-water data than in a directly measured deepwater spectra. A single shallow-water directional buoy or slope array is therefore less desirable for estimating deepwater, incident wave conditions than direct deepwater measurements, particularly for long-period swell.

Short-period waves are usually characterized by a broad directional distribution and undergo less refraction than low-frequency waves in the same water depth. Therefore, directional buoys in coastal waters may resolve directional distributions of seas better than swell. However, generation by local winds can cause the energy of these high-frequency waves to have much more rapid spatial variations in deep waters compared to the lower frequencies. Including high-frequency waves in a regional network requires both monitoring (or modeling) of the spatially variable wind field and the inclusion of source terms in the wave propagation model. This is beyond the scope of the present report.

Inverse Methods

Numerical simulations with spectral wave models indicate that, with complicated bathymetry, estimates of coastal wave conditions can be very sensitive to errors in the shape of the deepwater directional spectrum. In this case, an offshore pitch-and-roll buoy is believed to be inadequate as a sole source of input to wave models (e.g., O'Reilly & Guza 1991). Routinely available spectral hindcasts also lack the required resolution for many coastal engineering applications. An alternative approach described here is to infer the deep-ocean directional spectrum from wave data collected in both deep and shallow water. Properly placed shallow-water gauges, used in conjunction with wave propagation models and (ideally) an offshore directional buoy, can significantly

improve regional wave estimates based on a single directional buoy (Chapter 3, section titled "Numerical Wave Models").

Wave measurements, even nondirectional measurements (i.e., energy), at specifically chosen locations, can constrain the possible shape of the incident deepwater directional spectrum. If an idealized coastal site were exposed to wave energy from a single, narrow range of deep-ocean directions and effectively sheltered from other directions (for example, a gauge situated shoreward of a gap between two islands), then the energy observed at that site would specify the deep-ocean directional spectra energy in the exposed directional sector. Observations from many such partially sheltered shallow gauges, each exposed to a different deep-ocean directional sector, could clearly be used to estimate the deep-ocean directional spectra. The governing assumption is that bottom effects are of highest priority and other effects modestly affect the spectrum. The collection of sheltered sites, each measuring energy alone, can be used to form a so-called "incoherent directional array." Directional wave information follows not from the phase information between closely spaced sensors (i.e. a conventional "coherent array"), but from the spatial variation of energy among the many spatially separated energy gauges. Because the effects of real bathymetry are more complex than the idealized "gaps" discussed above, estimating the deep-ocean directional spectrum from shallow-water measurements is vastly more complicated. So-called "inverse methods," developed for conceptually similar problems in geophysics and other disciplines, provide the necessary mathematical framework. Given a numerical wave propagation model, and a set of wave measurements (either directional and/or nondirectional) obtained in either shallow water alone or in both shallow and deep water, the inverse method described below yields an estimated deepwater spectrum that is "consistent" with these observations. Thus, wave monitoring through inverse methods ideally includes both a deepwater directional buoy and shallow-water gauges.

An objective means of estimating the "information content" of a specific network of gauge locations is an integral part of the inverse approach to wave monitoring. Inverse methods can thus be used not only to extract regional wave information from a given network, but also to design networks. Combined with an optimization technique known as simulated annealing, inverse methods can be used to determine how many gauges are necessary to define specific regional wave parameters, and to select locations that maximize the amount of useful (i.e. non-redundant) wave data collected with a fixed number of gauges. The inverse approach thus quantitatively links network design and performance.

4 Southern California: A Case Study of the Inverse Method

This chapter describes how inverse methods and an existing 10-year database of measurements by the CDIP in the Southern California Bight (Figure 1) can be used to estimate the deep-ocean directional spectra. Estimated peak directions are compared to hindcast directions for a few example wave events. These estimated offshore spectra could in turn be used as input to the wave models to estimate extreme wave conditions throughout the Bight during the last decade. This example illustrates how inverse methods can be used with an existing database of wave measurements to estimate historical wave conditions at unmeasured sites. In addition, a method for designing optimal networks for inverse modeling is presented. Data from an optimal network, recently deployed in Southern California, are presently being used to test the inverse method of designing and using regional wave networks (O'Reilly & Guza, in preparation).

The inverse method of network design requires a wave propagation model. The two models used here, spectral refraction (R Model, Longuet-Higgins (1957)) and spectral refraction-diffraction (RD model, Kirby (1986)), are fully described in O'Reilly & Guza (1992). Both models assume that the deep-ocean spectrum is spatially homogeneous outside the Bight, and that there is no local wave generation or dissipation. Thus, the models are limited to the estimation of Bight-wide wave conditions associated with swell from distant storms.

Linear Programming (Non-Negative Least Squares)

Mathematical techniques, broadly defined as inverse methods, can be used with the wave models and data collected in the Bight to estimate deep-ocean directional spectra (see O'Reilly (1991) for details). The term "forward model" will refer here to either the R (refraction) or RD (refraction-diffraction) wave model. For a given wave frequency, the forward model yields a linear relationship between the deep-ocean directional spectrum S_o and the wave
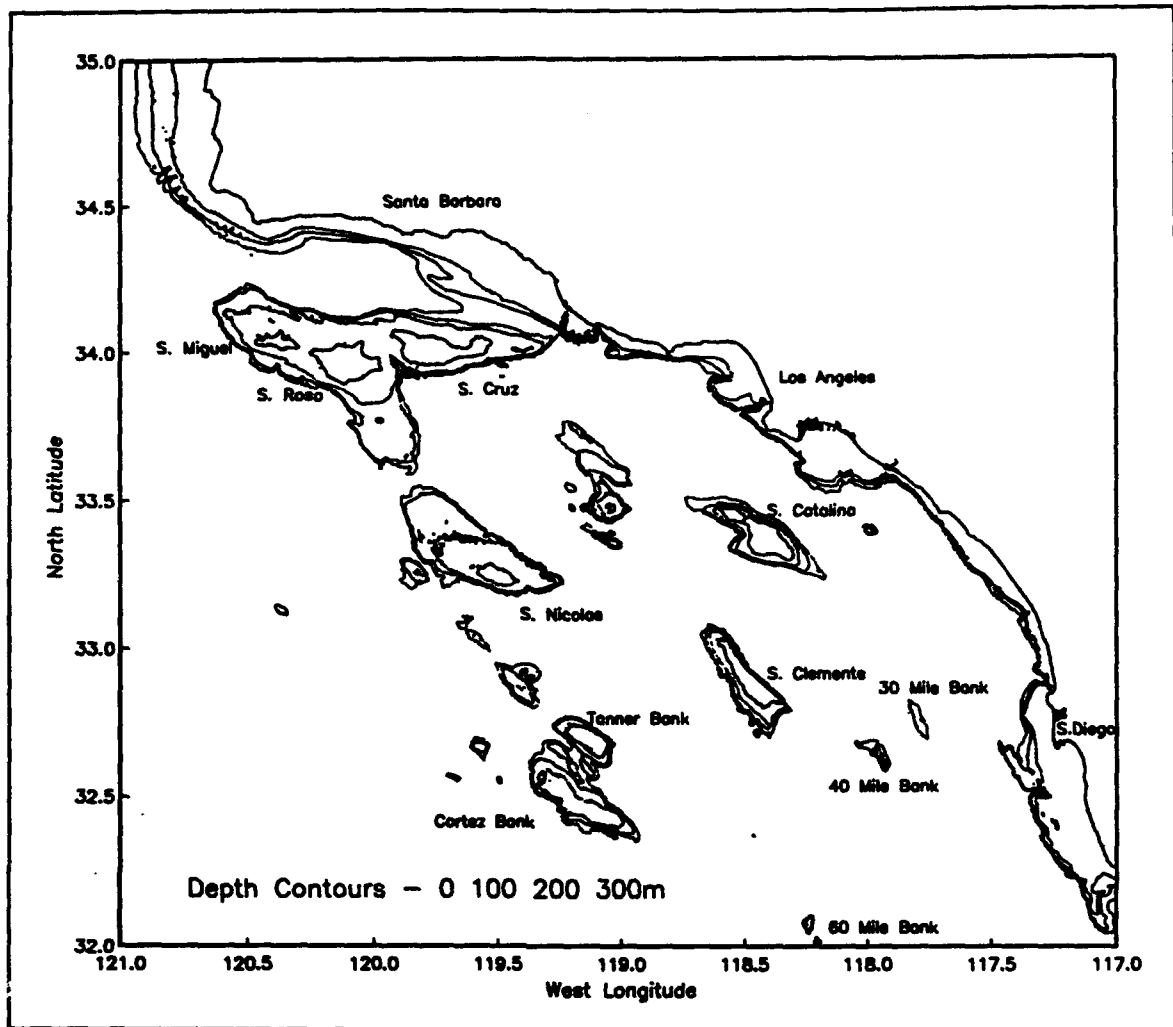
Figure 1. Shallow-water bathymetry of the Southern California Bight

measurements d (energy or directional moments, for example), which can be expressed as a linear functional of S_0:

$$d(x) = \int_\theta d\theta\, G(x,\theta)S_0(\theta) \tag{1}$$

G is derived from the forward model, and is essentially a shoaling-refraction-diffraction transfer function (O'Reilly & Guza 1992).

Further simplification reduces Equation 1 to a linear programming problem. Instead of seeking a function form, the solution S_0 is discretized into a finite number of frequency-directional bins, each with constant wave energy density. The problem is then reduced to the matrix form

$$Ax = b \tag{2}$$

where

$b = b_1, b_2, \cdots;$

$b_M = $ the observations

$x = x_1, x_2, \cdots$

$x_N = $ the discretized deep ocean spectrum, at a fixed frequency

$A = $ M by N matrix composed of the forward model energy or directional transfer functions for each wave measurement

$A_{ij} = $ the forward model estimate of some wave parameter, say energy, at observation site i due to a unit amount of wave energy arriving from the deep-ocean direction bin j

A numerical program well-suited for this particular inverse problem, NNLS (Non-Negative Least Squares, *Lawson and Hanson* (1974)), finds the non-negative deep-ocean spectrum that provides the best least squares fit to the observations.

$$NNLS = \frac{min}{\chi \geq 0} |A\chi - b|^2 \tag{3}$$

The length M of the data vector b is the number of individual observations available in the Bight at a given time. The length N of the solution vector x is the number of directional bins for the discretized deep-ocean spectrum. A frequency bandwidth of $.01 Hz$ and a directional bandwidth of 5 deg are used here, and the range of possible incident deep-ocean wave directions is assumed to be between 160 deg and 315 deg ($N = 36$). Since the forward model is linear, there is no transfer of energy between frequencies, and each $.01\text{-}Hz$ band can be treated as a separate inverse problem.

When using historical wave observations, the inverse problem is often poorly constrained (i.e. $M \ll 36$). To ensure a unique solution, an a priori smoothness constraint is added to the linear programming problem by specifying that the difference between neighboring directional bands equals zero. The kernel A and the observations b are expanded to include these additional constraints:

$$A_{M+j,j} = w_d; \quad A_{M+j,j+1} = -w_d; \quad b_{M+j} = 0, \text{ for } j = 1, N-1 \tag{4}$$

where w_d is a weighing factor that forces the NNLS routine toward directionally smoother solutions as w_d increases, and the remaining elements in each row are set to zero. This results in a total of $M + N - 1$ data constraints and the problem is over-determined if $M > 1$. The NNLS routine finds the solution that results in the best least squares fit to the data and smoothness constraint, and w_d controls the relative penalty of observation misfits versus lack of

smoothness. The use of a directional smoothness constraint does not eliminate the possibility of narrow solutions. Inverse model simulations with both narrow and broad spectra suggest that a properly weighted smoothness constraint can improve the overall inverse model performance without seriously degrading the solutions for narrow spectra. These simulations are discussed further in the section of this chapter titled "A Qualitative Comparison of Inverse Estimates and Deep-Ocean Wave Hindcasts."

Modeling Nonstationary Wave Events

The time required for wave energy to propagate between spatially separated wave measurement stations in the Southern California Bight (Figure 1) can be as long as 6 hr for a wave frequency of .05 Hz and 14 hr for .10-Hz waves. For a given frequency band, the time lag between any two stations theoretically depends on the wave direction, and observed time lags are qualitatively consistent with expectations. For example, westerly storm wave energy arrives and wanes at the offshore gauge before the nearshore gauges. Observed time lags at the beginning and end of large wave events thus contain additional information about the wave directions in deep water.

Travel times between observation sites and temporal nonstationarity in the deep ocean spectrum are incorporated into the inverse model by simultaneously solving for many temporally sequential directional spectra. A wave measurement at a specific site and a given frequency band is now linearly related to different directional bins of the deep-ocean spectra at different times. Time lags for each frequency-directional combination, at each site, are approximated using simple geometry as illustrated for waves from the west (270 deg) and a deep-ocean location at 33 deg, 120 deg W (Figure 2). For a given wave frequency, the distance of wave propagation d_p between the deep-ocean site and an observation station is divided by the deepwater group velocity to get a time lag estimate (rounded to the nearest hour for the discretized inverse problem).

The time lag approximation is somewhat crude since the distance d_p is the shortest path the waves could take (and often an impossible one due to island blocking). Island sheltering generally results in multiple, less direct, arrivals from a single incident direction. In addition, the decrease in wave speed with depth is not accounted for. As a result, there is a bias towards underestimating lag times. A more accurate time lag approximation could be made using the travel time of back-refracted rays in the R model. However, a more sophisticated estimation scheme is pointless here because the lags are discretized to the nearest hour and wave data are typically collected 3-6 hr apart.

The nonstationary inverse problem can also be expressed as a linear functional
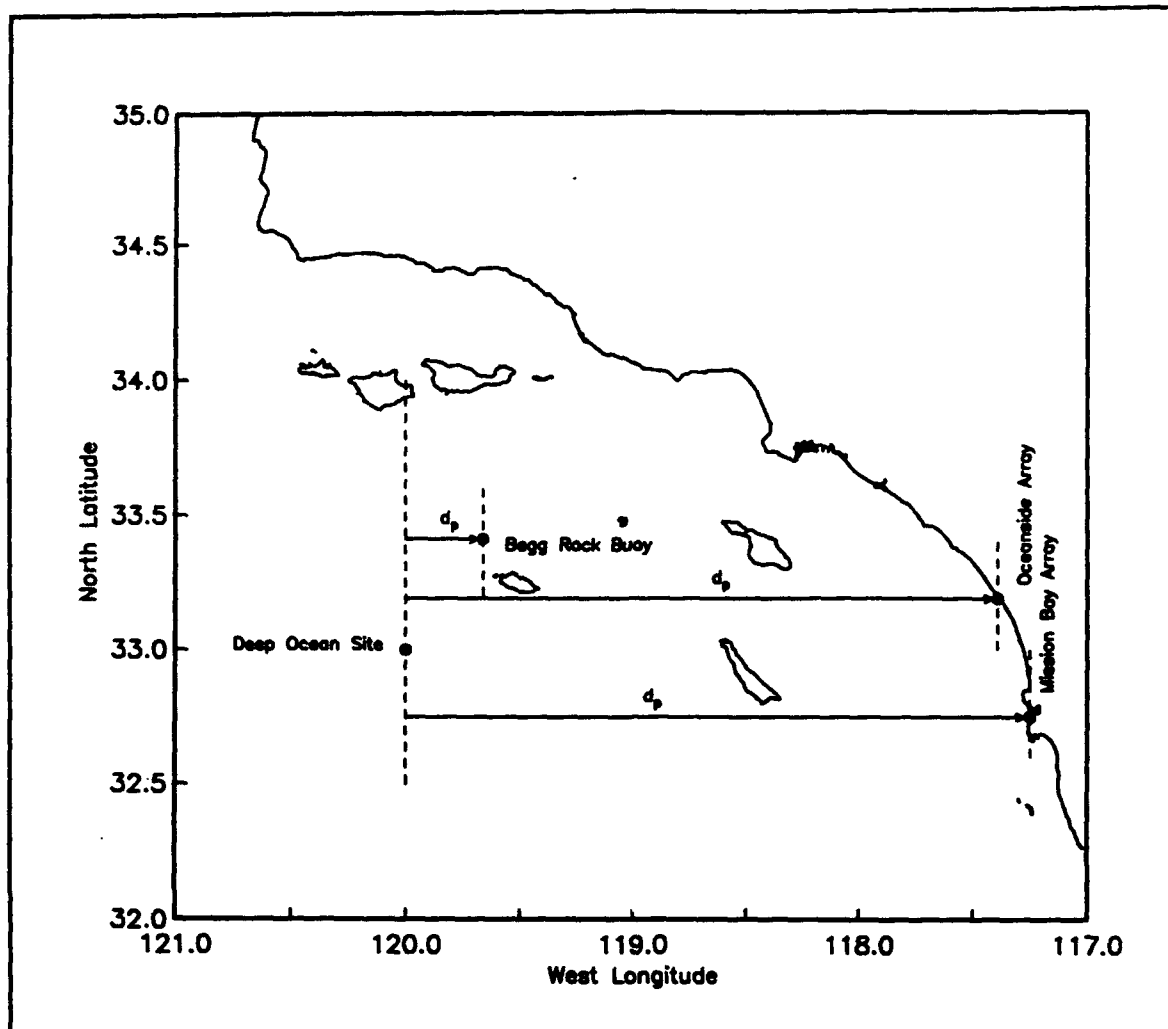
Figure 2. Geometry for estimating the distance between two points in order to calculate wave propagation time lags. Incident wave direction is 270 deg (i.e. from the west)

$$d(x,t) = \int_\theta \int_t d\theta dt \; G(x,\theta,t) \; S_0(\theta,t) \tag{5}$$

where d, G and S_0 now have the additional dimension of time. The kernel A of the discretized problem (Equation 2) now relates the forward model estimate at one observation location to deep-ocean spectra over a range of hourly time bins. The dimensions of A, excluding any smoothness constraint, increase from M by N to L by kN, where k is the number of hourly deep-ocean spectra solved for simultaneously and L is the number of wave observations made within that time period. $A_{i, hj}$ is the contribution of a unit amount of wave energy from deep-ocean direction j, at hour h, to the wave observation i. Unless hourly wave observations are made, the addition of the time domain makes the problem even less data-constrained than the stationary wave energy case. However, the inverse model can be constrained to have smooth solutions in time (with a corresponding weight, w_s) as well as direction. A is a large, sparse matrix when both smoothness constraints are included. For example,

Chapter 4 Southern California: A Case Study of the Inverse Method

solving for a 36-hr time period of incident wave spectra results in roughly a 2,600 by 1,300 matrix inversion problem.

Observations from the Coastal Data Information Program

The Coastal Data Information Program has been collecting wave data in the Southern California Bight since the late 1970's [*Seymour, Sessions, and Castel* 1985]. These data have been collected at numerous locations throughout the Bight using either pressure sensors or Waverider (nondirectional) buoys (Figure 3). The shallow-water stations are generally at a depth of 10 m and often provide directional information using a slope array of four pressure sensors. The majority of the slope array data were collected at 6-hr intervals, and the buoy data every 3 hr, with each data record about 17 min long at a 1-Hz sample rate. Recently, the record lengths have been increased to a sample size of 34 min or more, and the 6-hr interval between sampling periods has been reduced in many cases. Over the last decade, NOAA has also operated several directional (pitch-and-roll) and nondirectional buoys in the region (Figure 3).

The Waverider buoys and single pressure sensors provide wave energy information only (i.e., one observation)

$$\int_0^{2\pi} E(f,\theta)\, d\theta$$

while the shallow-water slope arrays and pitch-and-roll buoys measure four additional directional moments (four "more observations") of the local wave spectrum (Longuet-Higgins et al. 1963).

$$\int_0^{2\pi} E(f,\theta)\cos\theta\, d\theta$$

$$\int_0^{2\pi} E(f,\theta)\sin\theta\, d\theta$$

$$\int_0^{2\pi} E(f,\theta)\cos 2\theta\, d\theta$$

$$\int_0^{2\pi} E(f,\theta)\sin 2\theta\, d\theta$$
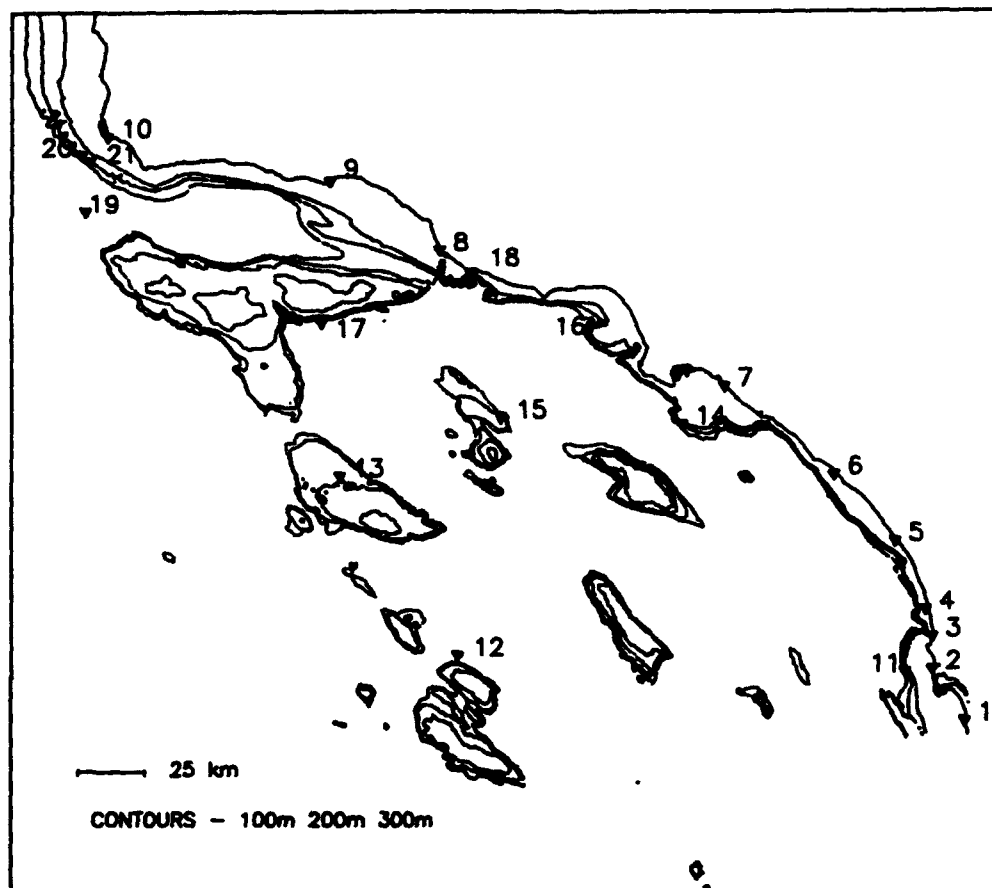
1 IMPERIAL BEACH ARRAY	12 NOAA BUOY 46024
*2 MISSION BAY ARRAY	*13 BEGG ROCK BUOY
*3 SCRIPPS PIER S.P.	14 SAN PEDRO CHANNEL BUOY
4 DEL MAR ARRAY	15 NOAA BUOY 46025
*5 OCEANSIDE ARRAY	16 SANTA MONICA BAY BUOY
6 SAN CLEMENTE ARRAY	17 SANTA CRUZ ISLAND BUOY
7 SUNSET BEACH ARRAY	18 POINT MUGU BUOY
8 CHANNEL ISLANDS S.P.	*19 NOAA BUOY 46023
9 SANTA BARBARA (2)	20 POINT ARGUELLO BUOY
10 POINT ARGUELLO BUOY	*21 HARVEST PLATFORM
*11 MISSION BAY BUOY	* = PRESENTLY OPERATING

Figure 3. Southern California wave observation stations, 1978 to present

Data used in the present study were processed from CDIP archive tapes and an estimation technique described by Herbers and Guza (1989) was used to calculate directional moments for the slope arrays.

A Qualitative Comparison of Inverse Estimates and Deep-Ocean Wave Hindcasts

Inverse model estimates of deep-ocean wave spectra, based on CDIP and NOAA wave data, were compared to deep-ocean wave hindcasts of a peak period and peak wave direction produced by Pacific Weather Analysis (U.S. Army Corps of Engineers 1988).[1] The peak directions of these hindcasts are fairly accurate since weather patterns that generate large waves are usually well-tracked. Two energetic Northern Hemisphere events (January 1985 and November 1989), and a single Southern Hemisphere swell event (August 1984) were examined. The CDIP and NOAA observation locations used in the inverse model are listed in Table 1 for each wave event. Three CDIP locations, Imperial Beach, Del Mar, and Scripps Pier, were excluded because of suspected inaccuracy and/or severe irregularity in the bathymetry grid.

Simulations were performed to select the directional smoothness weight w_d to use in the actual inverse model calculations. For simplicity, the inverse simulations were based on stationary test spectra. These "true" spectra were used to create "data" using a forward wave model and chi-square statistical noise (20 degrees of freedom) was then added to the data to simulate 17-min wave records with the appropriate resolution. The simulated data were in turn used in the inverse model to estimate the original test spectra. The simulations were performed for the .055- to .065-Hz frequency band and with the observation stations that were operating during each event (Table 1).

The overall objective is to use inverse methods along with a forward wave model to make Bight-wide wave estimates. To select a directional smoothness weight, a measure of the "goodness" of the inverse solutions, using Bight-wide estimates of wave heights, was defined. For each test case, the true and estimated deep-ocean spectra were used with the RD model to predict the wave height (H_{rms}) at roughly 4,000 locations spaced 3,200 m apart across the Bight. The root mean square error between the true and estimated wave heights was then calculated for each of four directional distributions (Figure 4). Thirty-six different simulations were performed by moving the center of the distribution in 5-deg increments from 160 deg to 315 deg. There were 50 different statistical realizations for each central direction, resulting in about 1,500 simulations at each of the 4,000 locations. The resulting H_{rms} errors were averaged to obtain a single representative value for each of the four directional distributions and a range of smoothness weights.

---

[1] Personal Communication, June, 1990, Nick Graham, Assistant Research Meteorologist, Scripps Institution of Oceanography, La Jolla, CA.

**Table 1
Observation Locations for Inverse
Estimates (See Location Map,
Figure 3)**

Date	Location
August 1984	Oceanside Array
	San Clemente Array
	Santa Cruz Island Buoy
	Begg Rock Buoy
January 1985	Mission Bay Buoy
	Oceanside Array
	San Clemente Array
	Santa Cruz Island Buoy
	Begg Rock Buoy
November 1989	Mission Bay Buoy
	Mission Bay Array
	Oceanside Array
	Sunset Beach Array
	Begg Rock Buoy
	Harvest Platform
	NOAA Buoy 46023
	NOAA Buoy 46025

The H_{rms} errors are plotted as a function of the smoothness weight w_d in Figure 5. Directionally broad test spectra produced lower H_{rms} errors and benefitted the most from the smoothness constraint. In addition, wave estimates for the narrow directional spectra (solid line, Figure 5) were not seriously degraded by a smoothness constraint large enough to be useful for broader spectra. The inverse estimates based on the January, 1985 wave observation network were more unstable than the other two examples, and improved to an H_{rms} error value similar to the August 1984 estimates when $w_d \leq .01$. Based on the simulations, $w_d = .1$ was chosen for use with the field data. In addition to the directional weight, a temporal smoothness weight of 1.0 was used. This is large enough to suppress large fluctuations in the inverse estimates on unrealistically rapid times of 1-2 hr, but small enough to not influence similar changes over 6-12 hr.

January 17, 1985

Northern Hemisphere winter storms typically form in the Northwest Pacific and travel eastward towards the Gulf of Alaska. Occasionally a storm takes a more southerly route towards the Hawaiian Islands and generates waves approaching the Southern California Bight from a more westerly direction. This was the case for a mid-January storm in 1985.

Inverse estimates of the deep-ocean directional spectra were made using the R model and the wave stations listed in Table 1 over a 36-hr time period starting at midnight on the 16th of January. The R model was chosen because its directional transfer functions could be used with the CDIP slope array data. Not including the smoothness constraints, there were a total of 79 observations of wave energies or directional moments to constrain the solution in 36 direction bins over 36 hr, or 1,296 direction-time bins. Figure 6 shows the non-stationary inverse model estimates of deep-ocean directional spectra, for the .055-.065 Hz frequency band (corresponding to the 17-sec peak period of the hindcast). The inverse estimate of the directional spectrum is consistent with the hindcast peak direction (267 deg) for this wave event. The peak direction for the .045- to 55-Hz frequency bank (Figure 7) starts at 260 deg and moves slightly northward to roughly 265-270 deg over a 20-hr period. This lower frequency wave energy arrives before the .06-Hz energy in Figure 6, typical of dispersive arrivals (lower wave frequencies travel faster) from distant storms.
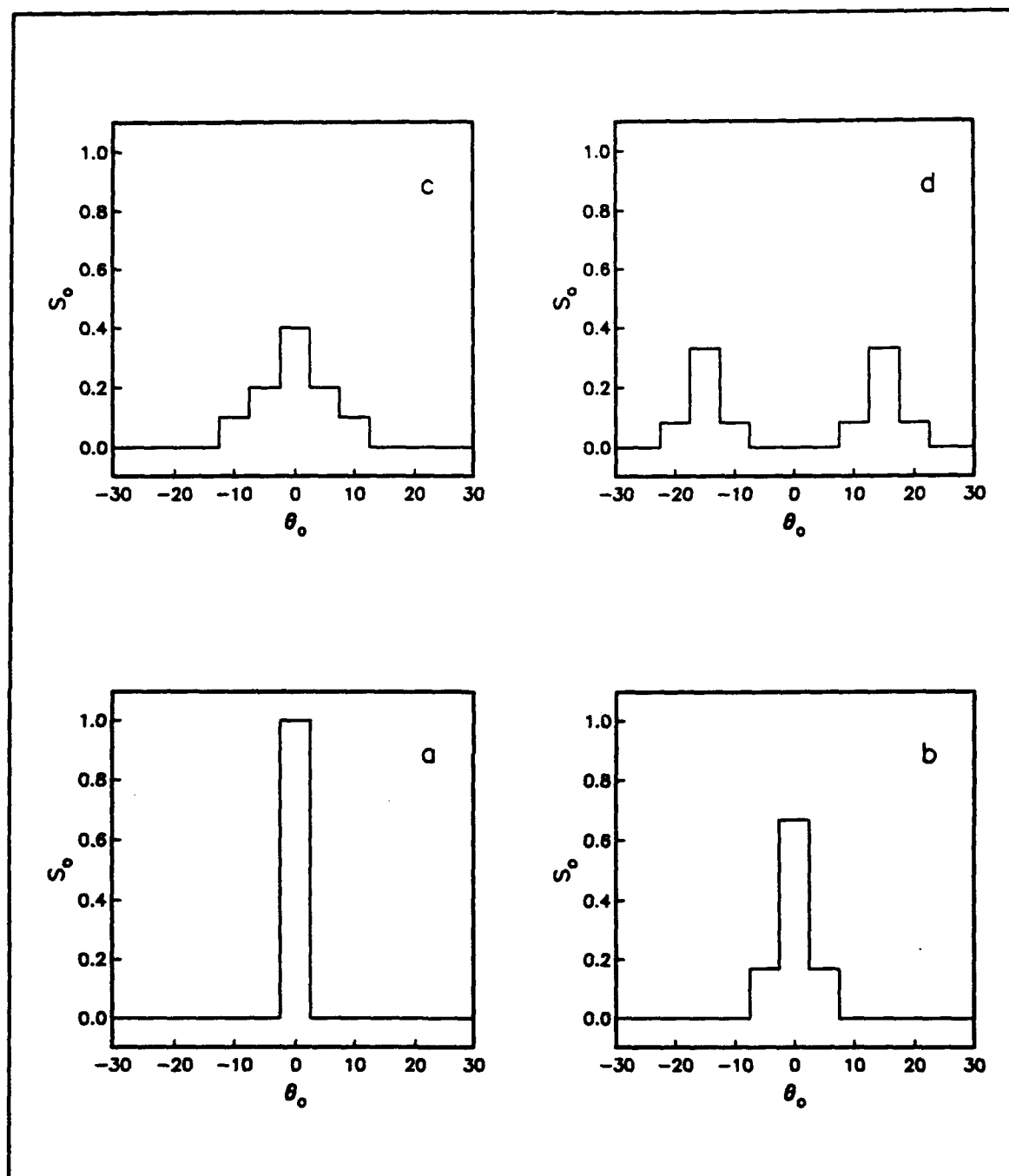
Figure 4. Test spectra for H_{rms} error simulations
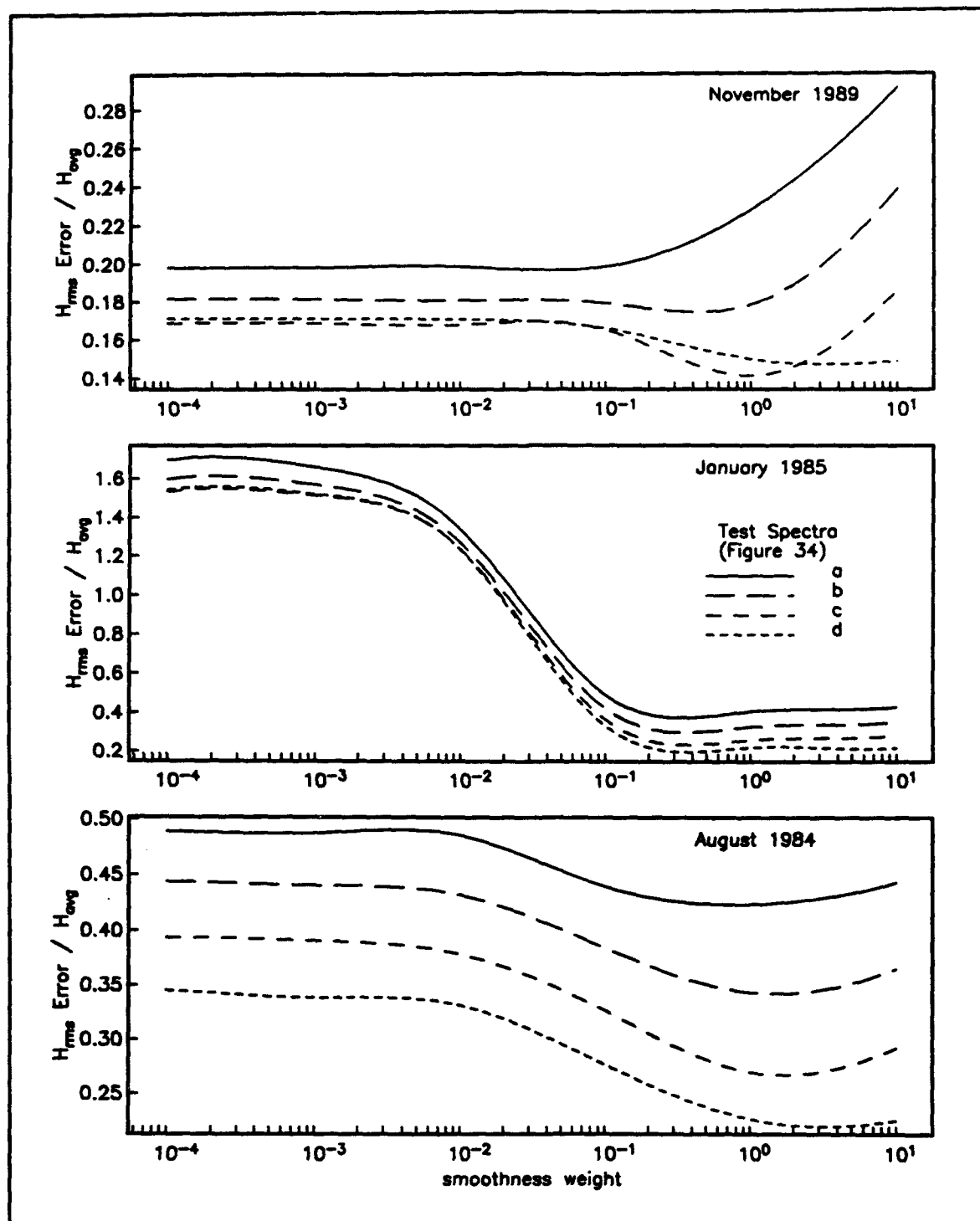
Figure 5. H_{rms} error as a function of directional smoothness weight w_d. Simulations assume that the deep-ocean spectrum is stationary
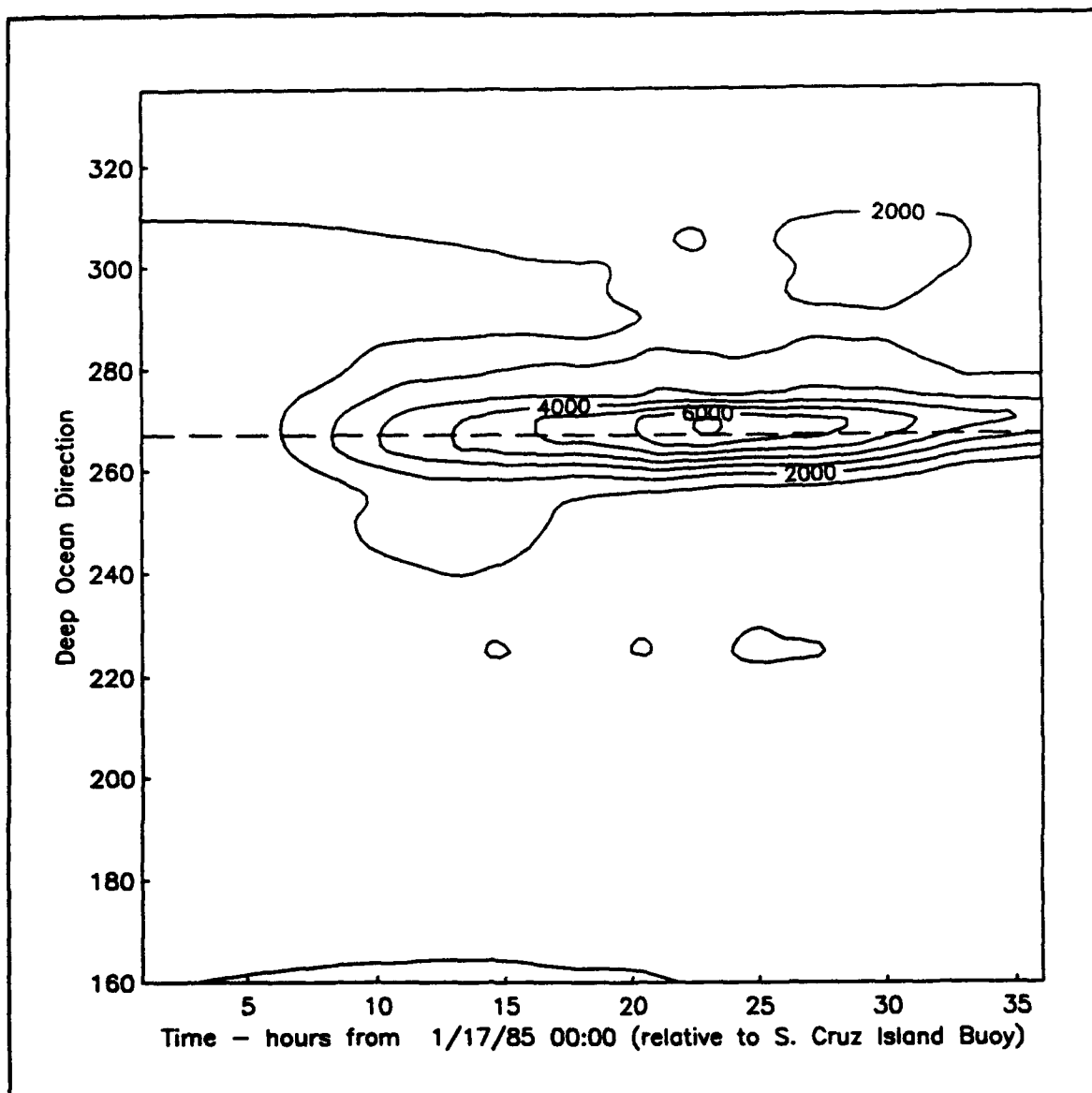
Figure 6. Inverse model estimate of the deep-ocean directional spectrum for a 36-hr time period beginning on January 17, 1985. The wave frequency band is .055 to .065 Hz. Contour levels of wave energy density are every 1,000 $cm_2/Hz°$. The dashed line represents the peak direction of the Pacific Weather Analysis wave hindcast
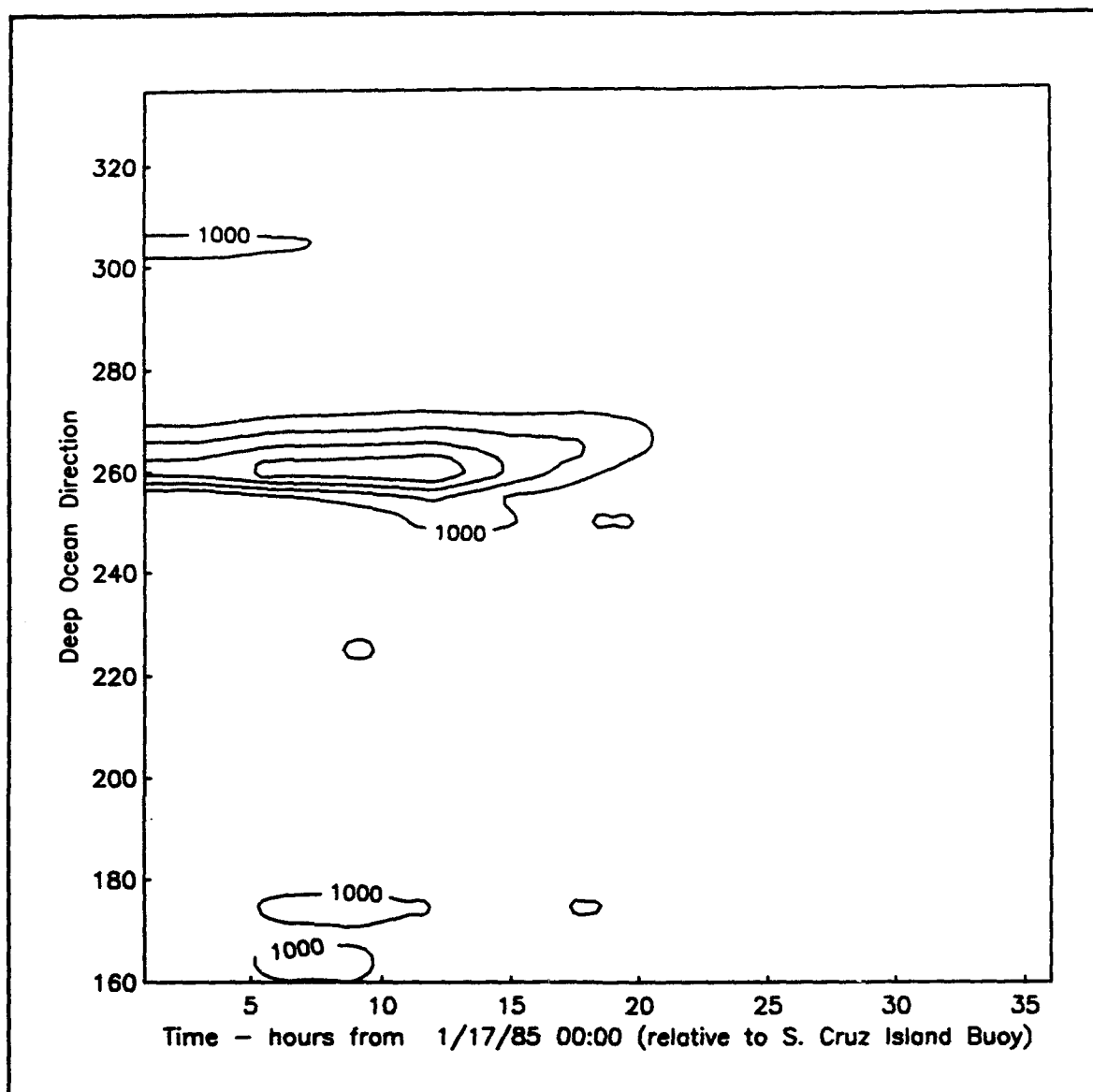
Figure 7. Inverse model estimate of the deep-ocean directional spectrum for a 36-hr time period beginning on January 17, 1985. The wave frequency band is .045 to .055 Hz. Coutour levels of wave energy density are every 1,000 $cm^2/Hz°$

November 3, 1989

On October 29-30, 1989, an exceptionally powerful storm developed in the far Northwestern Pacific with wave energy reaching Southern California on the 3rd of November. This storm was unusual because the wave frequencies containing the greatest amount of energy were .05 Hz and lower. A relatively large number of wave observat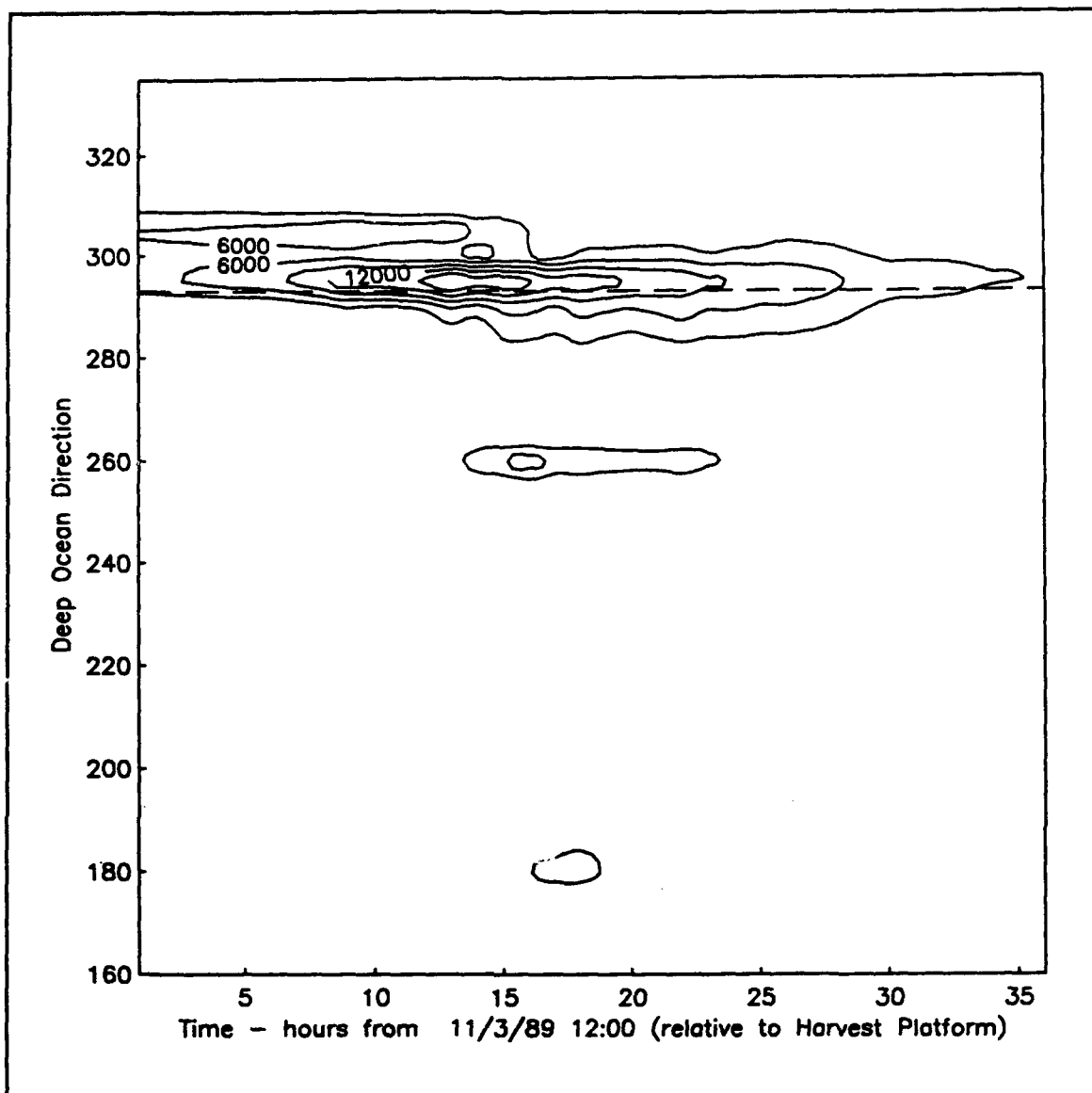ions were available for this event, and six CDIP stations and two NOAA buoys (Table 1) were used in the 36-hr inverse estimate for the .045- to .055-Hz frequency band (Figure 8). The R model transfer functions were used with the CDIP data and the RD model energy transfer functions for the NOAA buoys. The peak direction in the inverse estimate was

Figure 8. Inverse model estimate of the deep ocean directional spectrum for a 36-hr time period beginning on November 3, 1989. The wave frequency band is .045 to .055 Hz. Contour levels of wave energy density are every 3,000 cm^2/Hz°. The dashed line represents the peak direction of the Pacific Weather Analysis wave hindcast

295 deg (recall that the deep ocean spectrum estimate was discretized into 5-deg bins), which is consistent with the Pacific Weather Analysis hindcast of 293 deg.

August 23, 1984

A less successful application of the inverse model was performed for a large Southern Hemisphere wave event in August, 1984, where the Pacific Weather Analysis hindcast estimated a peak period of 17-18 sec and direction of 198 deg. The R model was used in the inverse problem along with four observation stations (Table 1). The inverse estimate for the .055- to .065-Hz frequency band is shown with the hindcast peak direction in Figure 9. The inverse model is inconsistent with the hindcast in this instance, generally showing bimodal directional spectra rather than a single peak.

Southern Hemisphere swells are generally assumed to be directionally narrow, and narrow spectra are the most difficult to accurately simulate with the forward models (O'Reilly and Guza 1992). Thus, it is interesting to explore whether or not the inconsistencies between the inverse model and the hindcast are primarily due to forward model errors. A different inverse estimate, one that assumes a priori that the incident spectra are directionally narrow, was also made using these wave observations. Instead of allowing the wave energy to be distributed across all 36 of the 5-deg deep-ocean directional bands, 36 separate inverse problems were solved. In each case the incident energy was constrained to a single 5-deg directional band for the 36-hr time period with the same temporal smoothness constraint $w_s = 1$. The resulting misfit between observations and estimates (Equation 3), a measure of how well the NNLS solutions fit the data, are plotted versus incident direction in Figure 10, upper panel. The overall minimum misfit, for the direction of 205 deg, is $657cm^4$ (compared to 528 cm^4 in the original inverse solution). The nonlinear inverse problem, with only a single directional bin, is actually over-determined by the data alone, and if the smoothness constraint is dropped altogether (Figure 10, lower panel), then the minimum misfit is $247cm^4$, for the direction 195 deg. Therefore, the inverse estimates (both with and without w_s) are quite consistent with the hindcast direction (198 deg), and the misfits are not much larger than in the full-nonstationary problem.

This analysis suggests that the forward model is not inaccurate, but rather the data set is fundamentally inadequate to define the offshore directional spectrum without rather drastic a priori assumptions (e.g., the wave field is directionally unimodal). Although some results are encouraging, the simple smoothness constraints in the full nonstationary inverse problem are inadequate in some cases, failing to even resolve the peak direction of a wave event. More information is needed to properly constrain the problem, either through additional observation, or a priori assumptions.
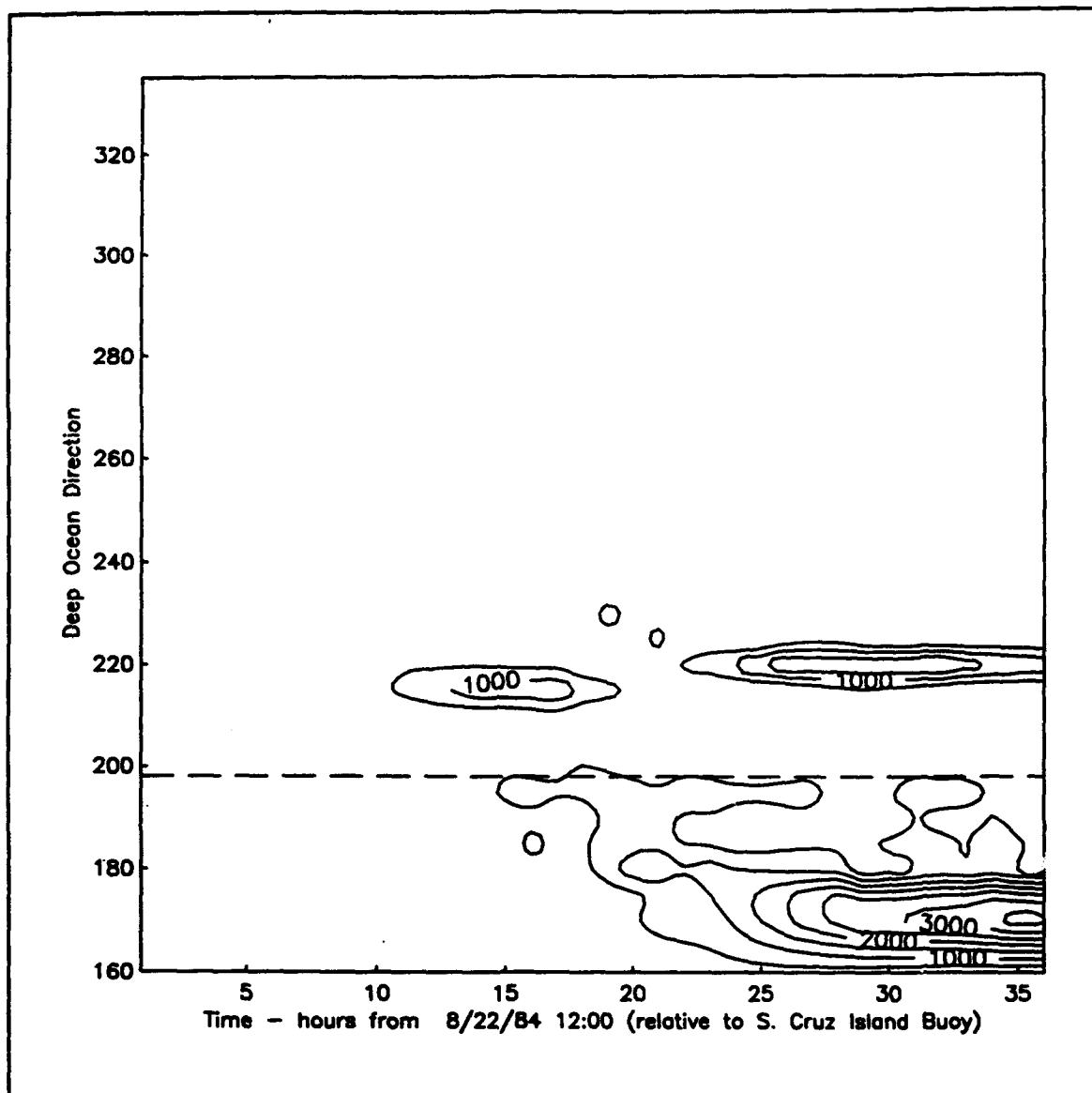
Figure 9. Inverse model estimate of the deep ocean directional spectrum for a 36-hr time period beginning at noon on August 22, 1984. The wave frequency band is .055 to .065 Hz. Contour levels of wave energy density are every 500 $cm^2/Hz°$

The hindcast information has been used here to check for inconsistencies in the inverse estimates. A hindcast could be used more directly in the inverse model, as a "preferred direction" constraint, for example, and spectral hindcast models could specify preferred shapes for the deep-ocean spectra. That is, a hindcast can be treated as "data" in the inverse model. An inverse estimate combining observations and hindcasts would presumably work best for extreme wave events since the location of distant sources of large waves is often well-known.
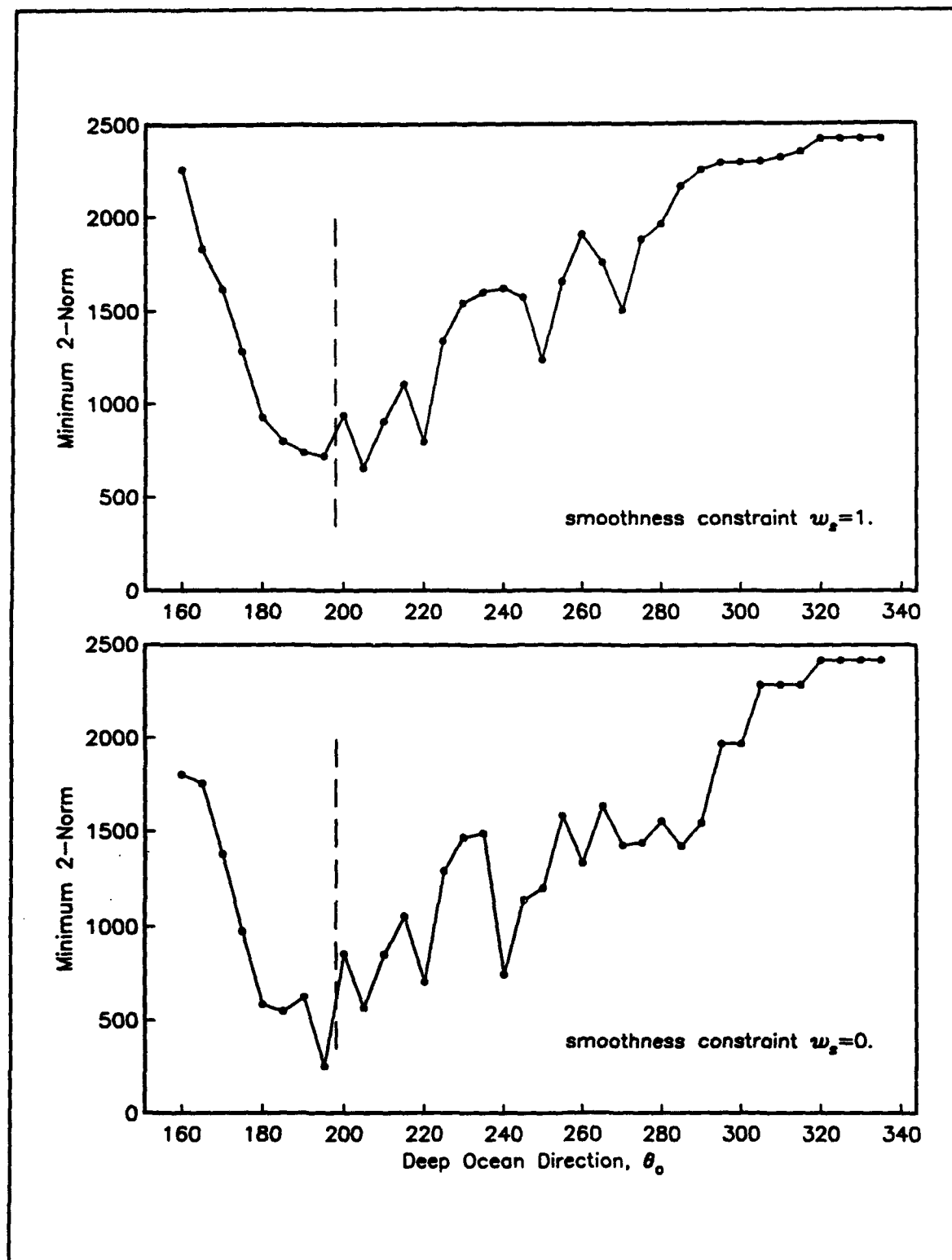
Figure 10. Minimum two-norm, or least square error, for the modified (a priori narrow incident spectra) inverse model. Each black dot represents the minimum two-norm for a 5-deg incident directional spectrum in the .055- to .065-Hz frequency band. The dashed line represents the peak direction of the Pacific Weather Analysis wave hindcast

5 Designing an Optimal Wave Data Network

Network Optimization by Simulated Annealing

Determining the deployment locations for a finite number of wave measurement instruments, in order to estimate wave conditions throughout the Bight, is a large combinatorial maximization problem. The quantity to be maximized is an objective function characterizing network performance. The number of possible network configurations in the Bight is enormous and the problem does not lend itself easily to simple optimization techniques.

Barth and Wunsch (1990) (hereafter B&W) use a method known as simulated annealing to design instrument arrays for acoustic tomography experiments. The present problem is analogous to theirs in almost every way, and is expressed in the same standard inverse form (Equation 2). The annealing method will be outlined only briefly since the objective function used here is that suggested by B&W, as is the general methodology for network selection.

Simulated annealing has its roots in thermodynamics and the technique of slowly cooling molten solids to form the most crystalline, lowest energy state possible. In order to achieve this, the cooling melt may have to go to higher energy states at various times, while still maintaining thermal equilibrium. The likelihood of a higher energy excursion of a given size ΔE decreases with temperature T and is governed by the Boltzmann probability distribution,

$$P(\Delta E) = e^{-\Delta E/T} \tag{6}$$

Metropolis et al. (1953) first incorporated Equation 6 into numerical calculations and the technique has more recently been used to solve the so-called traveling salesman problem (Press et al. 1986). In simulated annealing problems, "temperature" becomes a parameter that controls how slowly the probability distribution function changes. In addition, ΔE refers to the difference in objective function values for two network configurations, one representing the current state of the system and the second being another possible configuration. Thus, new configurations with worse objective function values are less

likely to be accepted at lower temperatures. Configurations with lower objective function values are always accepted.

In simulated annealing, a random combination of M locations is selected and an initial objective function value is calculated. The network is then modified or "jumped" to a different configuration in a random way. A new objective function value is calculated for this network and the new configuration is accepted or rejected with a probability given by Equation 6. To change the network configuration, a wave station in the network is randomly selected and moved to another site that is also randomly chosen. However, the maximum distance of this random move decreases with the system's temperature. This iterative process continues for a chosen rate of decreasing temperature, which is referred to as the annealing schedule, until no further configurations are accepted (based on specified iteration and temperature thresholds).

B&W suggest an objective function based on the singular value decomposition of the kernel A in Equation 2. Small singular values correspond to elements of the inverse solution x that will be seriously degraded by forward model errors in A and statistical errors in b. By maximizing the *smallest* of the singular values of A, the overall sensitivity of the inverse problem to these errors is minimized.

To guarantee reaching a global minimum (or a global *maximum* if the minus sign in the exponent in Equation 6 is dropped) the rate at which the temperature can be decreased is extremely slow and often computationally unrealistic. However, investigators have found that much faster annealing schedules can be used in many cases, with results that are at least near-optimal if not the global minimum. Because simulated annealing cannot always guarantee convergence to a global minimum, its use as a true optimization technique is somewhat controversial. At the very least, simulated annealing can provide good solutions to combinatorial optimization problems where one's intuition is normally quite limited. Whether or not the solution is truly optimal is a question of theoretical interest; however, in practice, it is unlikely that the objective function to be minimized will embody all aspects of the actual problem in the first place. Thus, for large optimization problems involving physical processes, the absolutely optimal solution may be sacrificed for a very good one that can be obtained at a fraction of the computational expense.

Optimized configurations, for networks of various sizes, are shown in Figures 11-12. In each case A did not include smoothness constraints and the Nth smallest singular value was maximized, where N is the number of stations in the network. The optimized locations are based on the energy transfer functions calculated by the stationary RD wave model for the .055- to .065-Hz frequency band. Approximately 17,000 sites were considered in the annealing problem, representing locations that were 1,600 m apart across the entire Bight. Note that several network sites are clustered together on the northwest edge of San Nicolas Island (Figure 1) in several cases (Figure 11). These sites are actually a few kilometers apart and lie along a spatial energy gradient associated with intense wave focusing. It appears that these locations were

Figure 11.   Energy transfer functions (lower panels) and station locations (upper panels) for optimized 8- and 12-station networks. Energy transfer functions are from the RD model for the .055- to .065-Hz frequency band
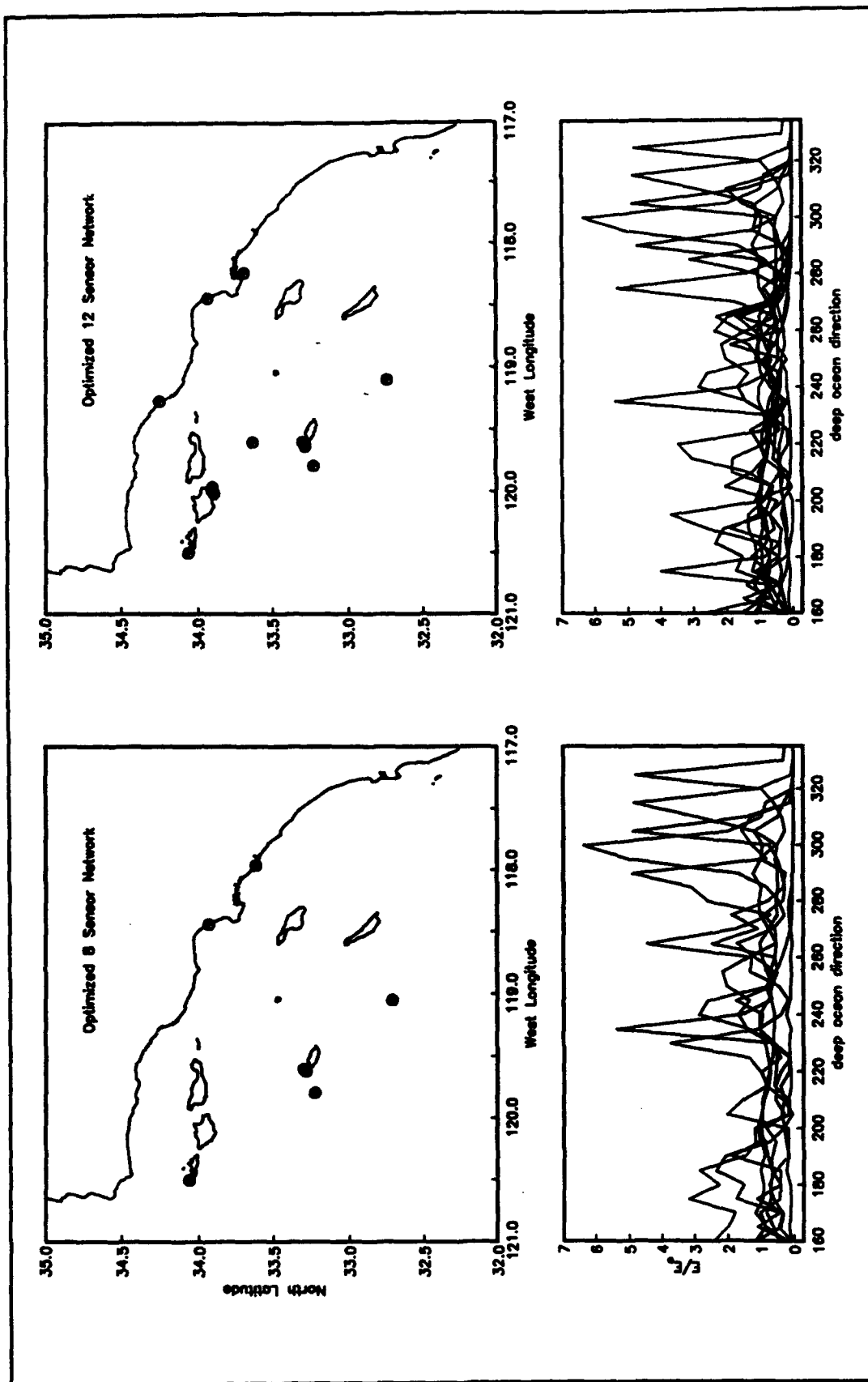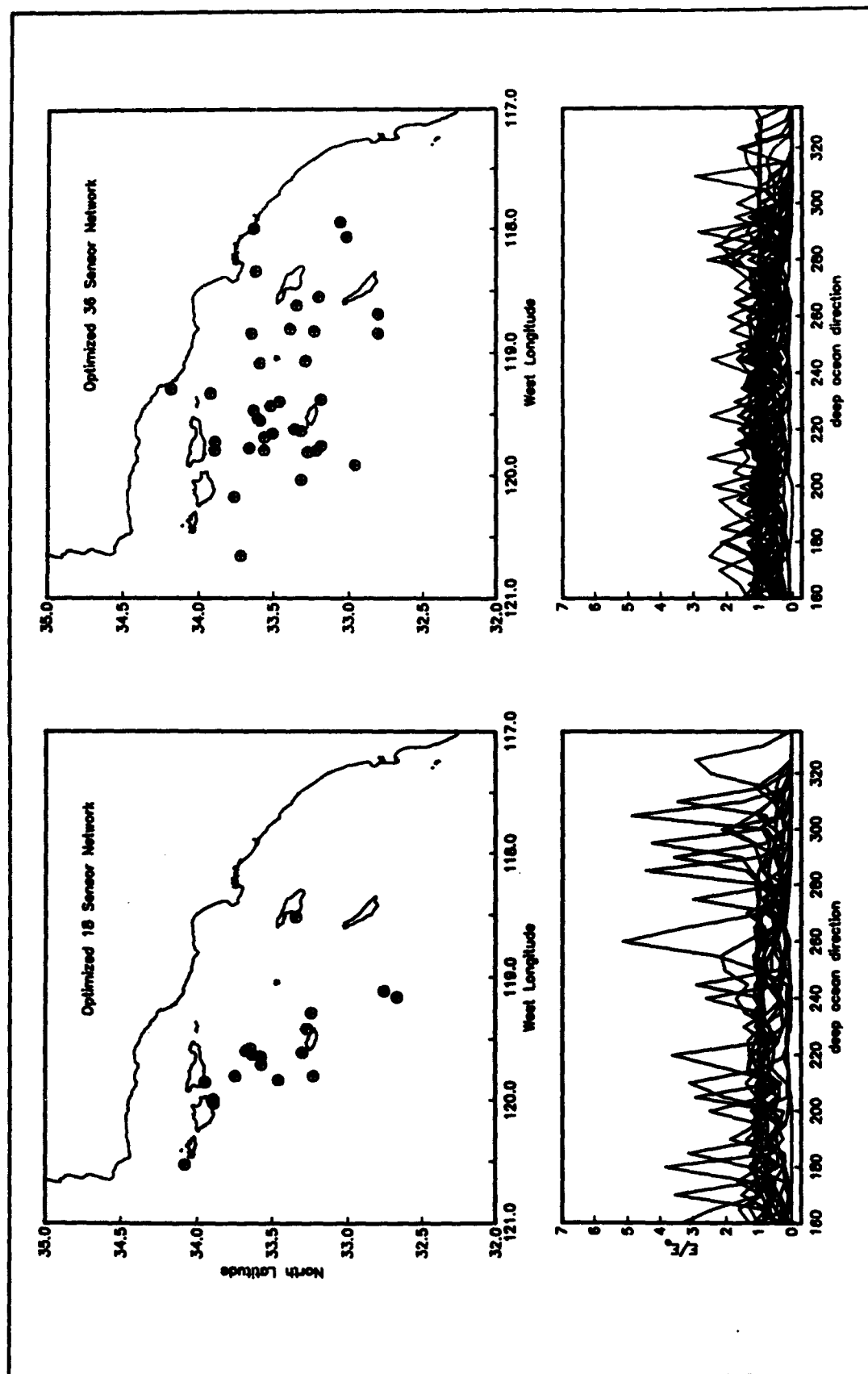
Figure 12.   Energy transfer functions (lower panels) and station locations (upper panels) for optimized 18- and 36-station networks. Energy transfer functions are from the RD model for the .055- to .065-Hz frequency band

chosen in an attempt to resolve wave energy from the northwest. The majority of the Bight is sheltered from these wave directions, hence the selection of sites outside the islands. Interestingly, the smaller networks seem to prefer larger energy transfer functions than the networks with more elements, resulting in more observation sites in shallow water for the sparse networks. The reasons for this are unclear at the present time.

The singular values for the 8-, 12-, and 18-station optimal arrays are shown in Figure 13. Also shown are the singular values for the networks used in the three wave events examined in the previous section. Although these wave events were estimated using only 4-8 stations, several of the stations provided directional moment measurements, which resulted in 4 additional model constraints in each case. The August 84, January 85, and November 89 events had a total of 12, 13, and 20 data constraints, respectively. The sizes of the singular values associated with the historical data networks are much smaller than those for the more optimal design. This indicates that there is a significant amount of redundancy in the existing wave data for these events. There is a fundamental trade-off in discrete inverse problems between solution resolution and stability. Relatively high directional resolution was sought here (5 deg), with what is in fact a minimal amount of wave measurement data, in the hope that the smoothness constraint would provide enough additional information to stabilize the solutions in the presence of model and data errors. However, this was clearly unsuccessful for the Southern Hemisphere swell in the section titled "August 23, 1984" in Chapter 4 (pages 22-24).

Simulations similar to those used in the previous section to select a directional smoothness constraint were also performed using optimal networks. Bight-wide H_{rms} error estimates, for the same test spectra of Figure 4, were calculated using the optimized 8-, 12-, and 18-station networks and various values of w_d (Figure 14). The smoothness constraint had less effect on the optimized networks, and the H_{rms} errors were smaller than those for the equivalent historical data networks (Figure 5).

The 12-station network was also used to examine changes in the H_{rms} as a function of forward model and statistical wave measurement errors (Figure 15, upper panel). As was done previously, chi-square errors were added to the simulated data before making the inverse estimates. It is difficult to characterize the type of forward model errors to be expected; therefore, the chi-square uncertainty is assumed to represent both model and measurement errors for the purpose of the present discussion. As would be expected, the H_{rms} error increases with decreased degrees of freedom. In addition, the size of the inverse model errors increases more rapidly at low degrees of freedom (<50). Finally, H_{rms} errors are calculated as a function of optimized network size (Figure 15, lower panel). The narrow test spectrum continues to result in the largest H_{rms} errors and there is a sharp increase in inverse errors between the 5- and 8-station optimized networks.
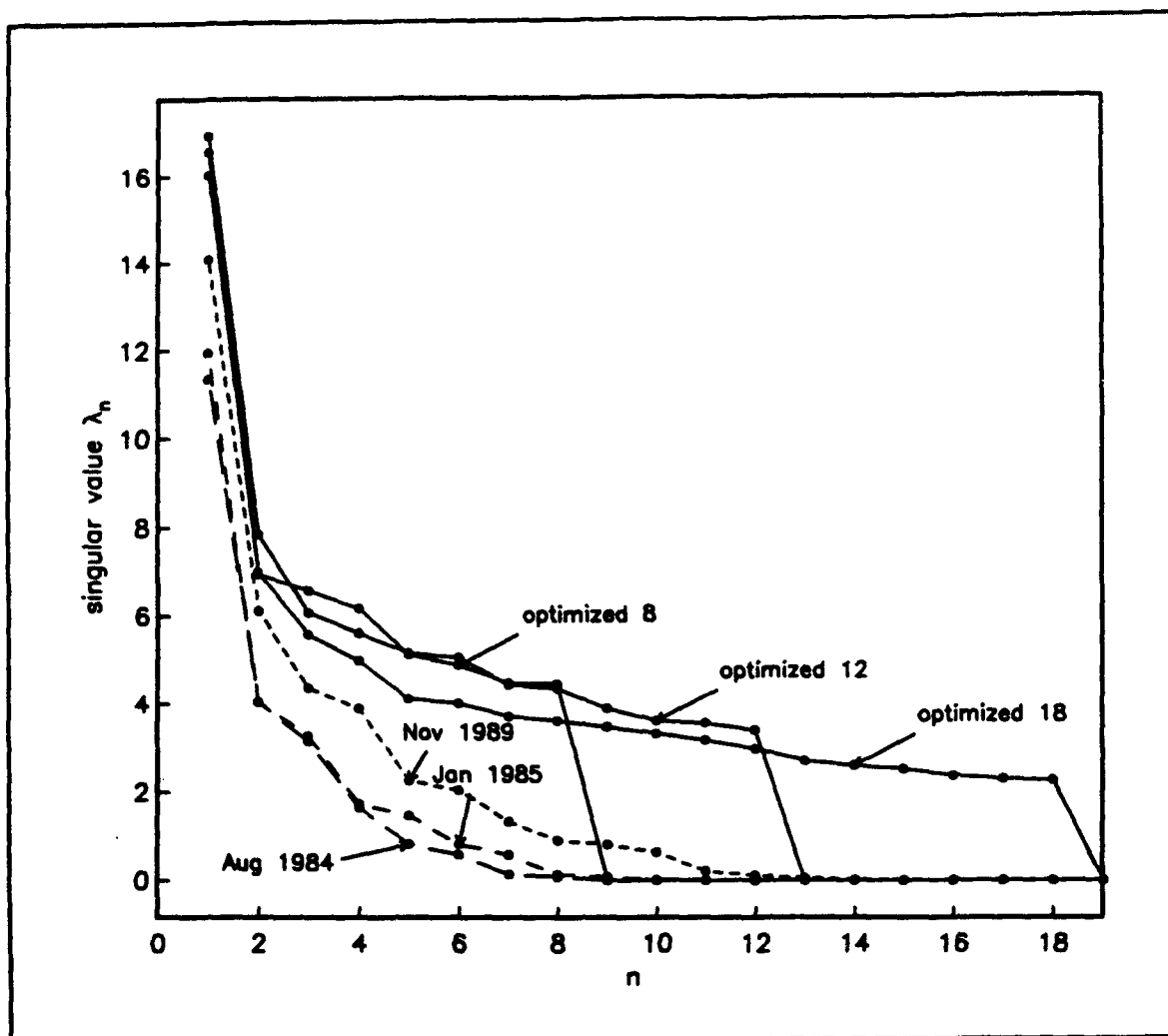
Figure 13. Singular values from the decomposition of the data kernels *A* for the historical wave networks and three optimized networks. Historical data kernels are based on the *R* model, and the optimized networks used the RD model. All data kernels are for stationary wave events in the .055- to .065-Hz frequency band

Discussion

In Chapter 4, a method was described to estimate nonstationary deep-ocean directional wave spectra, that in turn could be used to predict wave energy and directional spectra throughout the Southern California Bight. These deep-ocean estimates are made using observations of wave energy and directional moments within the Bight, along with linear programming techniques.

Examples of this inverse estimation method were presented using historical wave data collected by CDIP and NOAA for several significant wave events.
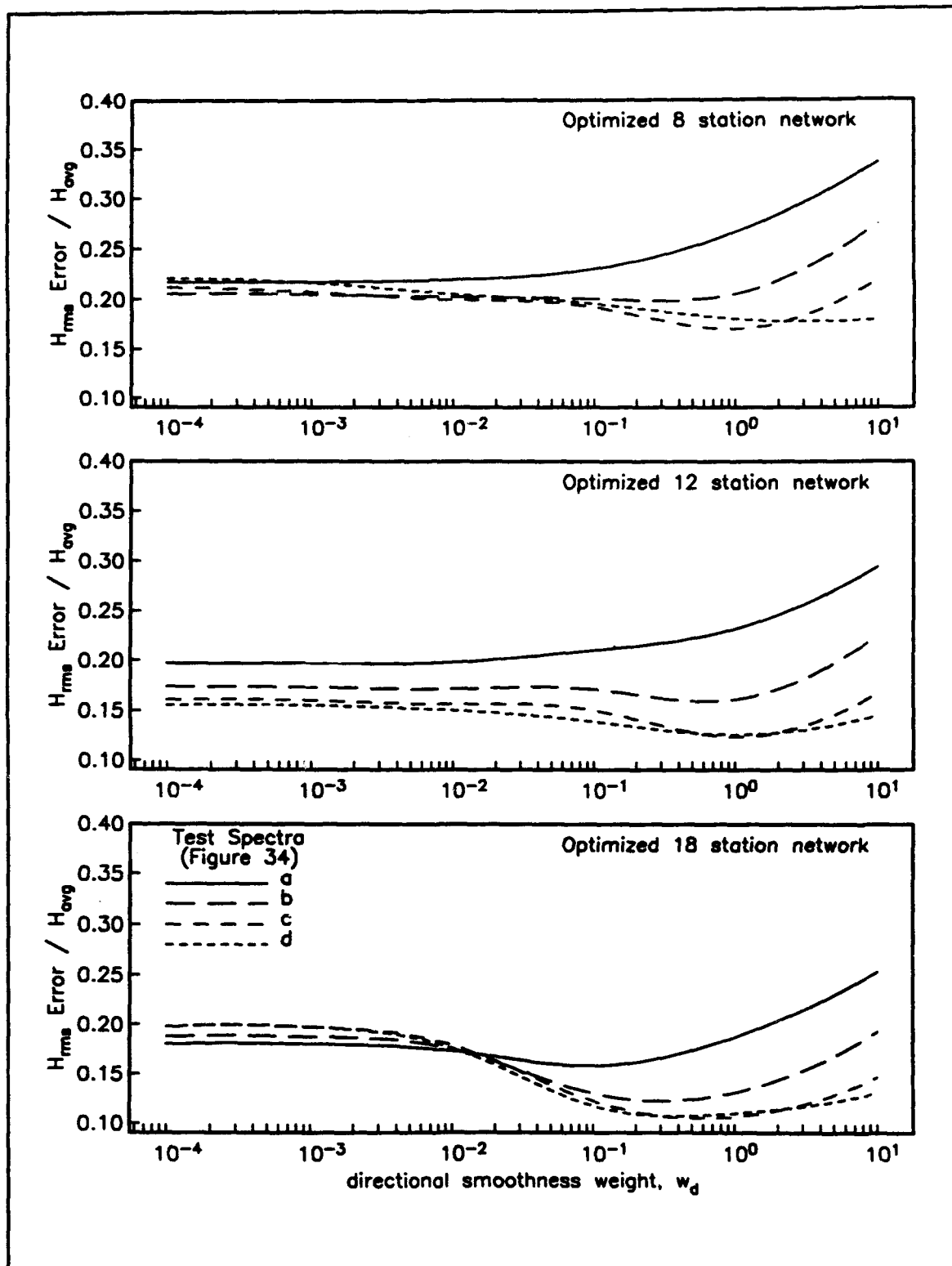
Figure 14. H_{rms} error as a function of smoothness weight w_d for the 8-, 12-, and 18-station networks. Simulations assume the measurements have 20 degrees of freedom
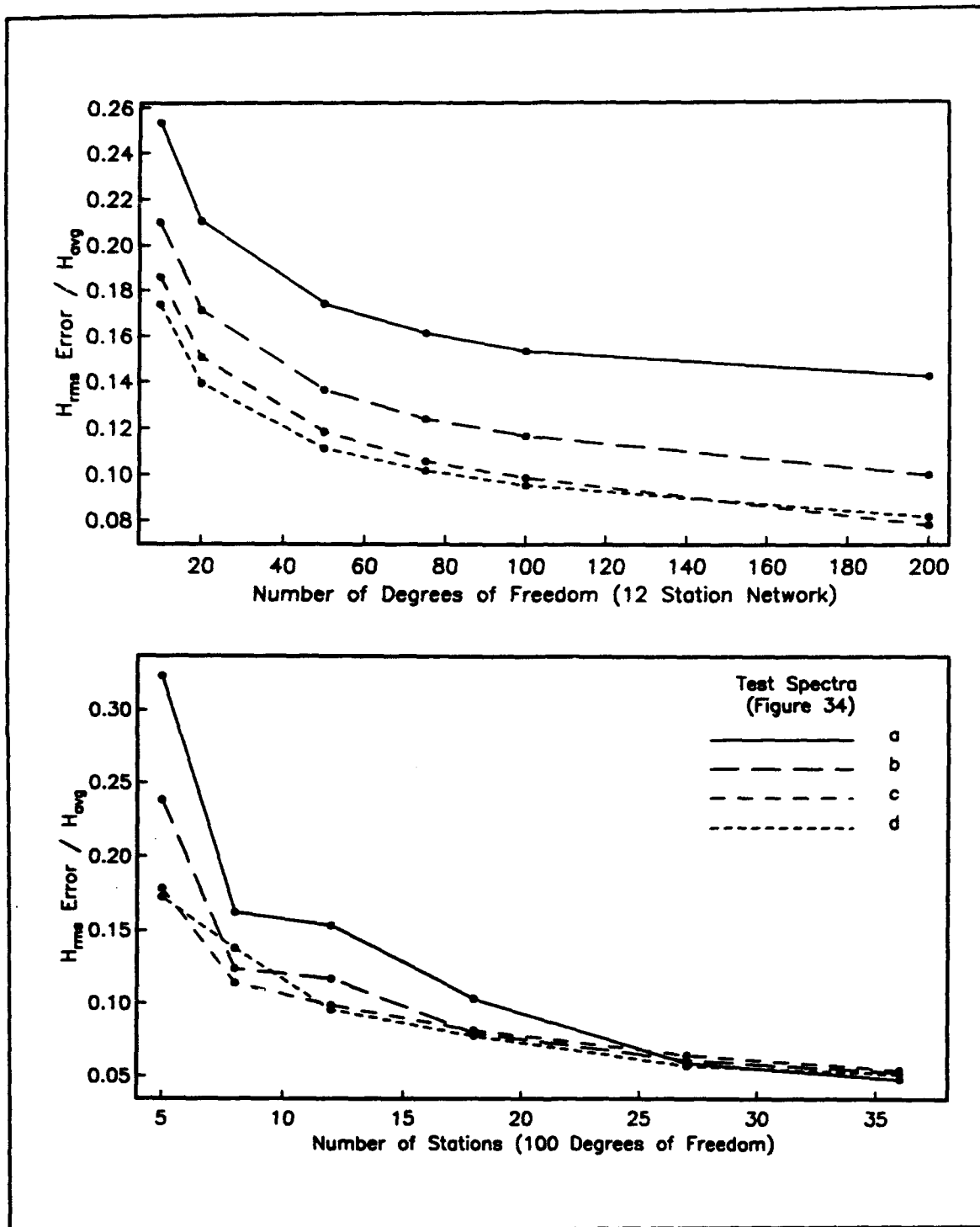
Figure 15. H_{rms} error as a function of optimized network size (lower panel) for wave energy measurements with 100 degrees of freedom, and H_{rms} error as a function of the number of degrees of freedom in the measurements for the 12-station network (w_d = .1)

Solutions were consistent with wave hindcasts in two cases, but not for the Southern Hemisphere swell event. A second estimation method, which assumed a priori that the incident spectrum was narrow, was also applied to the southern swell, and produced much better results. This suggested that, although narrow incident spectra are the most difficult for the forward models to simulate, the R model was reasonably consistent with the hindcast and observations in this instance, and more information was needed to constrain the problem.

More optimal wave networks, designed using simulated annealing, demonstrated that significant improvements could be made in the inverse estimates if the observation locations were tailored specifically for this task. Yet, even when they are optimized, the smaller networks suffer from a lack of information. Although the larger optimal networks shown may not be economically feasible, they do provide insight into some aspects of designing a practical network for inverse modeling. For example, if optimized locations are being used, a directional smoothness constraint is of limited benefit. In order to improve solution stability, more information (observations or hindcasts) must be added.

Alternatively, the number of deep-ocean directional bins might be reduced. As mentioned previously, the fundamental tradeoff in inverse problems is resolution versus stability of the solution. Here, a directional resolution of 5 deg was chosen, but less resolution could be considered, say 15 deg. This would reduce the number of unknowns to as few as 12 for a given hourly time period and therefore lead to more stable estimates. However, if incident wave spectra are truly narrow, then more serious forward model errors would result. Another possibility is to vary the size of directional bins based on a priori assumptions. For example, significant wave energy rarely comes from the directions 235-255 deg, so this range of incident angles could be treated as a single directional bin, or perhaps excluded completely. In addition, swell arriving in the Bight that is generated in the Northern Hemisphere is believed to be directionally broader than swell generated in the Southern Hemisphere; and little energy from incident directions greater than 310 deg propagates into the Bight. Thus, it may be possible to treat some of these west-northwesterly directions with wider directional bins and reduce the number of unknowns without seriously degrading the usefulness of the estimates.

A six-month field experiment (August, 1991 to February, 1992) has been completed to assess the viability of more optimal networks. Ten individual pressure sensors were deployed to temporarily expand the present CDIP and NOAA wave network. These self-contained, bottom-anchored instruments measured wave energy and were powered and recorded data internally. The experiment was separated into two 3-month deployments with the first deployment designed to observe Southern Hemisphere swell, and the second tailored to Northern Hemisphere events. In the optimized networks shown (Figures 11-12), simulated annealing was allowed to select shallow-water locations, and did so in the smaller networks. However, the forward model solutions are considered to be better in deeper water, away from locally strong refractive and diffractive effects. In addition, the largest bathymetry errors are most

likely to be found in shallow regions. Therefore, the instrument of choice would be deepwater Waverider or pitch-and-roll buoys; however, the cost of these instruments is somewhat prohibitive. Instead, a "poor man's" optimal network, made up of the low-cost pressure sensors, was deployed in a water depth of 30 m. This depth was selected in an attempt to minimize the forward model errors, while remaining shallow enough for recovery by scuba divers to be possible. A ten-station expansion of the present network is consistent with what is essentially a cost benefit curve, shown in Figure 15.

When speculating about a permanent network for inverse estimation, pitch-and-roll buoys are particularly appealing because they provide five observations at one deepwater location. However, from an inverse estimation perspective, a fair amount of redundancy/instability would result in comparison to individual energy measurements. In other words, a data kernel based on optimally moored pitch-and-roll buoys will always have smaller singular values, and less stability, than the kernel for a network consisting of five times as many optimally placed Waverider (energy only) buoys. Nevertheless, these smaller singular values may be tolerable when weighed against economic and logistical factors.

6 Conclusions and Recommendations

Conclusions

For regions with simple shelf and nearshore bathymetry, straightforward linear interpolation between coastal measurement sites may be acceptable for monitoring swell. However, if the bathymetry is simple enough for such a procedure, then many coastal observations might be replaced with a single offshore directional wave buoy coupled with a numerical wave propagation model.

In bathymetrically complex areas, coastal swell conditions are more spatially variable, and are also more sensitive to the details of the frequency-directional distribution in deep water. Simple correlations between wave measurements at different sites are not likely given the range of possible deep-water wave conditions. Interpolation schemes are thus not economically viable because a very large number of instrument stations would be required.

Numerical wave models, used in conjunction with directional buoys and shallow-water wave measurements, appear to be a necessary element in a cost-effective regional monitoring network. Field verification of these models has been difficult because of the need for moderately high-resolution deepwater directional spectra. A recent field experiment in Southern California, co-sponsored by the California Department of Boating and Waterways, Sea Grant, and the U.S. Army Corps of Engineers, was designed to test these models using offshore buoy data to initialize the models. In addition, a directional array of sensors was deployed on Harvest Platform, 100 km offshore from Point Conception, CA, in the 200-m water depth, in the fall of 1992. This array will provide slightly higher resolution deep-ocean directional spectra than those obtained with a pitch-and-roll buoy, and will contribute further to the verification of future numerical wave prediction schemes.

If it is found that pitch-and-roll buoys cannot provide high enough resolution deep-ocean information in some regions, then inverse methods could use both deep- and shallow-water wave measurements to better resolve the incident directional spectra. This method is presently undergoing verification in Southern California.

One of the results of this inverse model study has been the development of an objective means for identifying optimal wave measurement locations, where optimal implies maximum information for defining the regional wave field. Given a specific number of instruments and the method to be used to estimate regional wave conditions, the optimization technique can provide the best locations for those wave measurements. Alternatively, the inverse method can be used to construct "cost-benefit" curves which describe the information content of an array versus the number of instruments deployed.

Generation of waves by local winds is an important and complicated process not included in the present discussion, which is restricted to low-frequency waves generated by distant storms. However, the inverse method can be used as a framework for the design of regional networks which incorporate local generation. If buoys are found to be adequate for monitoring swell in a specific region, then shallow-water instrument locations could be tailored to monitor local seas.

Recommendations

An important question in the future planning of a U.S. wave monitoring program is how well coastal wave conditions can be predicted from a deep-water directional buoy and existing numerical wave models. The answer to this question will govern the relative mix of deep- and shallow-water stations in an optimal wave monitoring program. Preliminary results from the southern California wave experiment on complex bathymetry suggest that offshore directional buoys may prove to be the monitoring method of choice for many sections of U.S. coastline. A number of directional buoys are operated by NOAA in the United States, and a search should be made for any corresponding shallow-water data that could be used to test numerical models in other less complicated regions throughout the United States.

The following recommendations are specifically aimed at trying to further understand swell waves, and optimal ways of monitoring them, in regions which have less complicated bathymetry than the Southern California Bight. It is recognized that a useful network must also monitor local seas. Very little research has been done on the topic of local seas and networks and this is clearly a subject that needs further study. A number of the following recommendations concerning the examination of existing data sets and new field studies (from the perspective of regional wave monitoring) could be expanded to include local seas.

In regions where no historical data are available, short-term field deployments of shallow-water gauges, in conjunction with a deepwater directional buoy, should be made. The network optimization method described in this report could be used to select shallow gauge sites which, owing to their lack of redundancy, provide the best test of the buoy/model method. Therefore, even if shallow-water networks are ultimately found to be less desirable than a

deepwater buoy for monitoring some coastal regions, optimal shallow-water gauge placement is still important for verification purposes.

If studies using historical data are successful, then the question of deep-water directional buoy spacing needs to be addressed. The most cost-efficient approach would be to use the WIS hindcast studies to estimate the spatial variability of the deepwater wave conditions along different regional coastlines, derive a desired spacing of buoys through numerical simulations with the wave models, and then verify the separation criteria through one or more regional field studies.

For complex coastal regions where directional buoys are inadequate, shallow-water measurements must be an integral part of the monitoring network. Much work on this topic has already been done in southern California and, if necessary, these methodologies can be applied to other complex coastal regions.

References

Barth, N., and Wunsch, C. (1990). "Oceanographic experiment design by simulated annealing," *J. Phys. Ocean 20*, 1249-63.

Herbers, T. H. C., and Guza, R. T. (1989). "Estimation of wave radiation stresses from slope array data," *J. Geophys. Res. 94 (C2)*, 2099-04.

Kirby, J. T. (1986). "Higher-order approximations in the parabolic equation method for water waves," *J. Geophys. Res. 91 (C1)*, 933-52.

Lawson, C. L., and Hanson, R. J. (1974). *Solving least squares problems.* Prentice-Hall, Englewood Cliffs, NJ.

Longuet-Higgins, M. S. (1957). "On the transformation of a continuous spectrum by refraction." *Proc. Camb. Phil. Soc.*, 53 (1), 226-9.

Longuet-Higgins, M. S., Cartwright, D. E., and Smith, N. D. (1963). "Observations of the directional spectrum of sea waves using a floating buoy." *Ocean wave spectra.* Prentice-Hall, Englewood Cliffs, N.J., 111-36.

Metropolis, N., Rosenbluth, M., Teller, A., and Teller, E. (1953). *J. Chem. Phys.* 21, 2245.

O'Reilly, W. C. (1991). "Modeling surface gravity waves in the southern California Bight," *Ph.D. diss.*, Scripps Institution of Oceanography, La Jolla, CA.

_____ (1992). "Data Report: The southern California wave experiment," SIO Ref. Ser. No. 92-14, Scripps Institution of Oceanography, La Jolla, CA.

O'Reilly, W. C., and Guza, R. T. "Comparison of spectral refraction and refraction-diffraction wave models," in preparation, *J. Waterway, Port, Coastal and Ocean Eng.*

_____. "A comparison of spectral wave models in the Southern California Bight," in preparation, *Coastal Engineering.*

Press, W. H., Flannery, B. P., Teukolsky, S. A., and Vetterling, W. T. (1986). *Numerical recipes.* Cambridge University Press, 818.

Seymour, R. J., Sessions, M. H., and Castel, D. (1985). "Automated remote recording and analysis of coastal data," *J. Waterway, Port, Coastal and Ocean Engineering 111 (2),* 388-400.

U.S. Army Corps of Engineers. (1988). "Historic wave and sea level data report: San Diego region," *CCSTWS 88-6.*

REPORT DOCUMENTATION PAGE

1. AGENCY USE ONLY (Leave blank)	2. REPORT DATE May 1994	3. REPORT TYPE AND DATES COVERED Final report

4. TITLE AND SUBTITLE
Design of Regional Wave Monitoring Networks: A Case Study for the Southern California Bight

5. FUNDING NUMBERS

6. AUTHOR(S)
William C. O'Reilly
David D. McGehee

7. PERFORMING ORGANIZATION NAME(S) AND ADDRESS(ES)
Scripps Institution of Oceanography, University of California,
San Diego, La Jolla, CA 92093
U.S. Army Engineer Waterways Experiment Station
3909 Halls Ferry Road, Vicksburg, MS 39180-6199

8. PERFORMING ORGANIZATION REPORT NUMBER

Miscellaneous Paper
CERC-94-11

9. SPONSORING/MONITORING AGENCY NAME(S) AND ADDRESS(ES)

U.S. Army Corps of Engineers, Washington, DC 20314-1000;
California Department of Boating and Waterways
1629 S Street, Sacramento, CA 95814-7291

10. SPONSORING/MONITORING AGENCY REPORT NUMBER

11. SUPPLEMENTARY NOTES

Available from National Technical Information Service, 5285 Port Royal Road, Springfield, VA 22161

12a. DISTRIBUTION/AVAILABILITY STATEMENT

Approved for public release; distribution is unlimited

12b. DISTRIBUTION CODE

13. ABSTRACT (Maximum 200 words)

Fundamental considerations in designing wave gauging networks, and an objective method for selecting optimal gauge locations for monitoring coastal wave conditions, are described. The focus is on the spatial variation of wave conditions owing to propagation across the continental shelf and near coastal bathymetry. Generation by local winds and dissipation within the surf zone are not included, so this preliminary work concerns nonbreaking, low-frequency swell waves. Application of the regional network design method is illustrated with an ongoing case study in the Southern California Bight, and the relevance of this work to other sections of the U.S. coastline is discussed. Recommendations for future studies, aimed at efficiently expanding the spatial coverage and, hence, utility of the present Field Wave Gauging Program are presented.

14. SUBJECT TERMS

Measurement	Optimization	
Model	Waves	
Network		

15. NUMBER OF PAGES
44

16. PRICE CODE

17. SECURITY CLASSIFICATION OF REPORT UNCLASSIFIED	18. SECURITY CLASSIFICATION OF THIS PAGE UNCLASSIFIED	19. SECURITY CLASSIFICATION OF ABSTRACT	20. LIMITATION OF ABSTRACT